# DDX60, a DExD/H box helicase, is a novel antiviral factor promoting RIG-I-like receptor-mediated signaling

Moeko Miyashita,[1,2] Hiroyuki Oshiumi,[1,*] Misako Matsumoto,[1] and Tsukasa Seya[1]

[1]Department of Microbiology and Immunology, Graduate School of Medicine, [2]Graduate School of Life Science, Hokkaido University, Kita-15, Nishi-7, Kita-ku Sapporo 060-8638, Japan

*Corresponding author. Mailing address: [1]Department of Microbiology and Immunology, Graduate School of Medicine, Hokkaido University, Kita-15, Nishi-7, Kita-ku Sapporo 060-8638, Japan. Phone: 81-11-706-5056. Fax: 81-11-706-7866. E-mail: oshiumi@med.hokudai.ac.jp

Running title: DDX60 is a novel antiviral protein

Key words: RIG-I, virus, type I interferon

Word counts for abstract: 165

Word counts for Materials and Methods: 1,937

Words counts for Introduction, Results, and Discussion: 4,304

Character counts for Introduction, Results, Discussion, and Figure Legend: 39,885

**ABSTRACT**

The cytoplasmic viral RNA sensors RIG-I and MDA5 are important for the production of type I interferon and other inflammatory cytokines. DDX60 is an uncharacterized DExD/H box RNA helicase similar to *S. cerevisiae* Ski2, a cofactor of RNA exosome, a protein complex required for the integrity of cytoplasmic RNA. The expression of DDX60 increases after viral infection, and the protein localizes at cytoplasmic region. After viral infection, the DDX60 protein binds to endogenous RIG-I protein. The protein also binds to MDA5 and LGP2, but not to downstream factors, IPS-1 and IKK-ε. Knockdown analyses shows that DDX60 is required for RIG-I or MDA5-dependent type I interferon and interferon-inducible gene expressions in response to viral infection. However, DDX60 is dispensable for TLR3-mediated signaling. Purified DDX60 helicase domain possesses the activity to bind to viral RNA and DNA. Expression of DDX60 promotes the binding of RIG-I to double-strand RNA. Taken together, our analyses indicate that DDX60 is a novel antiviral helicase promoting RIG-I-like receptor mediated signaling.

## INTRODUCTION

RIG-I and MDA5 are cytoplasmic viral RNA sensors belonging to the group of RIG-I-like receptors (RLRs), which includes LGP2 (57-59). RIG-I recognizes RNAs from vesicular stomatitis virus (VSV), hepatitis C virus (HCV), Sendai virus (SeV), and influenza A virus (21, 36, 37), while MDA5 recognizes RNA from picornaviruses such as encephalomyocarditis virus and poliovirus (PV) (3, 19, 21). RLRs are also involved in the recognition of cytoplasmic B-DNA. RNA polymerase III transcribes cytoplasmic AT-rich double-stranded DNA (dsDNA), and the transcribed RNA is recognized by RIG-I (1, 6). In contrast, Choi *et al* have reported that RIG-I associates with dsDNA (7).

When RIG-I or MDA5 is activated by viral infection, the N-terminal caspase recruitment domains (CARDs) associate with the adaptor protein IPS-1 (also called MAVS/Cardif/VISA) on the outer mitochondrial membrane (22, 26, 42, 55). After this association occurs, IPS-1 activates TBK1 and IKK-ε, and signals interferon (IFN) regulatory factor-3 (IRF-3) and NF-κB-responsive genes, such as type I IFNs or other inflammatory cytokines (22, 23, 26, 42, 44, 55).

Both the helicase and C-terminal domain (CTD) of RIG-I bind to RNA, but it is CTD that is responsible for the recognition of the 5' triphosphate double-stranded structure typical of viral RNA (16, 39, 40). Recently, Rehwinkel *et al* showed that the physiological ligand of RIG-I during influenza A or SeV infection is the full-length viral genomic single-stranded RNA (ssRNA), which possesses base-paired regions or defective interfering "DI" genomes (35). In contrast to RIG-I, MDA5 recognizes long double-stranded viral RNA (21). The RNA binding activity of the MDA5 CTD is

relatively weak compared with that of the RIG-I CTD, because the basic surface of the MDA5 CTD has a more extensive flat than the RIG-I CTD (8, 45, 46). Although the RNA binding activity of the MDA5 CTD is weak, this protein plays a pivotal role in the recognition of picornavirus RNA (20, 21).

For the efficient recognition of viral RNA, RIG-I and MDA5 require the protein modification and the association with upstream factors. LGP2 is one of the upstream factors. LGP2 lacks an N-terminal CARD: thus, the LGP2 itself cannot transmit the signal in the absence of RIG-I or MDA5 (36, 38, 49). The CTD of LGP2, which binds to the terminal region of viral double-stranded RNA, is more similar to the CTD of RIG-I than to that of MDA5 (24, 33, 45). LGP2 knockout studies have revealed that LGP2 is essential for type I IFN production by MDA5 but plays only a minor role in type I IFN production by RIG-I (38, 49). RIG-I requires modification of K63-linked polyubiquitination by TRIM25 and Riplet/REUL ubiquitin ligases for its full activation (11, 13, 30, 31). High mobility group box (HMGB) proteins also act as upstream factors of RLRs. Recently, Taniguchi and his colleagues reported that the HMGB1-3 serve as sentinels for the nucleic acids required for both RIG-I and MDA5 recognition of viral RNA (56). Takaoka and his colleagues reported that ZAPS associates with RIG-I to promote oligomerization and ATPase activity of RIG-I (15). Another factor interacting with RLRs is DDX3, a DExD/H box RNA helicase, which is similar to LGP2 in that it does not contains a CARD, but promoting signaling by forming a complex with either RIG-I or MDA5 (32). DDX3 also plays important roles in TBK-1 and IKK-ε-mediated IRF activation, and Schroder et al. and Soulat et al were the first to describe that DDX3

is a non-RLR helicase involved in innate immune responses (41, 43).

DDX60, a DExD/H box helicase, was annotated in a genome project, and the protein function is unknown. The protein is weakly similar to SKIV2L and SKIV2L2, and is the human homolog of *Saccharomyces cerevisiae* (budding yeast) Ski2, a cofactor of the RNA exosome (9, 18). The RNA exosome is a macromolecular protein complex that includes ribonucleases and helicases, and controls the quality of host RNA molecules in both the nucleus and cytoplasm (17). It is composed of nine core components and several cofactor proteins (18). In budding yeast, the RNA exosome and Ski2 together exhibit antiviral activity (53, 54): similarly, the mammalian RNA exosome with its cofactors show antiviral activity against Moloney leukemia virus and Sindbis virus (5, 14). Our microarray analysis has shown that DDX60 is upregulated in human dendritic cells during infection with measles virus (MV) (our unpublished results). Thus, we expected DDX60 to be a novel antiviral protein, and found that DDX60 is involved in RIG-I-like receptors-dependent antiviral pathway.

Here, we show that DDX60 is induced during viral infection and suppresses viral replication. DDX60 was found to form a complex with RLRs, promoting signaling: knockdown experiments indicate that DDX60 is involved in RLRs-dependent pathway. Moreover, the DDX60 helicase domain was observed to bind to viral RNA and DNA. Furthermore, DDX60 is required for type I IFN expression after DNA virus infection. These data indicate that DDX60 is a novel antiviral helicase involved in RLRs-dependent pathway.

## MATERIALS AND METHODS

### *Cell Cultures*

HEK293 and Vero cells were cultured in Dulbecco's modified Eagle's medium with 10% heat-inactivated fetal calf serum (Invitrogen), and HeLa cells were in minimum Eagle's medium with 2 mM L-glutamine and 10% heat-inactivated fetal calf serum (JRH Biosciences). HEK293FT cells were maintained in Dulbecco's modified Eagle's high glucose medium containing 10% heat-inactivated fetal calf serum (Invitrogen). Raw264.7 cells were cultured in RPMI 1640 medium with 10% heat-inactivated fetal calf serum (Invitrogen). Mouse bone marrow derived dendritic cells were induced as described in (2). PVR transgenic mice were provided by Koike (Tokyo Metropolitan Institute for Neuroscience).

### *Plasmids*

The full-length human DDX60 cDNA was obtained from HeLa cell total RNA by RT-PCR. The obtained cDNA fragments were sequenced, and we confirmed that the obtained cDNA clones do not contain nucleotide mutation by PCR. The DDX60 cDNA clone was cloned into *Xho*I-*Not*I restriction sites of pEF-BOS, and HA-tag sequence was inserted just before the stop codon. EXOSC1, EXOSC4, or EXOSC5 was amplified by RT-PCR from HeLa cell total RNA. The obtained cDNA fragment was cloned into *Xho*I-*Not*I restriction sites of pEF-BOS vector, and the FLAG-tag was fused at the C-terminal end. The DDX6 cDNA encoding full-length ORF were amplified by RT-PCR using primers; DDX6-F: GGC CGC TCG AGC CAC CAT GAG CAC GGC

CAG AAC AGA G and DDX6-R: GGC GGG GTA CCC CAG GTT TCT CAT CTT CTA CAG. The fragment was cloned into *Xho*I and *Not*I sites of pEF-BOS vector. For in vitro viral RNA synthesis, we amplified VSV-G region cDNA by PCR using primers VSV-G-F and VSV-G-R. The obtained cDNA fragment was cloned into pGEM-T Easy vector. The primers sequences are as follows; VSV-G-F, ACAGGAGAATGGGTTGATTC and VSV-G-R, ATGCAAAGATGGATACCAAC. RIG-I full or partial fragment expressing vectors are described before (30). The plasmids expressing TLR3 or TICAM-1 are described in (29). p125luc reporter plasmid was a gift from Dr. T. Taniguchi (University of Tokyo, Tokyo, Japan). Mutant DDX60 expression constructs were amplified using primers DDX60(1-169),(169-334),(334-490),(478-656),(657-857),(857-1054),(1049-1256),(1256-1409),(1407-1543),(1543-1712). The primers sequences are shown in supplementary Table I.

***Phylogenetic analysis***

The amino acid sequences of the DExD/H box domain were aligned using the ClustalW software on the NIG server. The phylogenetic tree was drawn by the neighbor-joining method of GENETYX-MAC (Version. 13.0.3.).

***Northern Blotting***

Human DDX60 644 bp cDNA fragment (from 3978 to 4621 bp region) was used for the probe for Northern blotting. The Northern blot membranes, human12-lane MTN blot

and MTN blot III, were purchased from Clontech. The probe was labeled with [α-$^{32}$P]dCTP using Rediprime II Random Prime labeling system (GE Healthcare). The labeled probe was hybridized to the membrane with ExpressHyb hybridization solution (Clontech) at 68 ℃ for 1h. The membrane was washed with washing solution I (2× SSC, 0.05% SDS) for 40 min, and washed with washing solution II (0.1×SSC, 0.1% SDS) for 40 min. DDX60 mRNA bands were detected with x-ray film.

***RT-PCR and Real Time PCR***

Total RNA was extracted with TRIZOL (Invitrogen), and then the samples were treated with DNaseI to remove the DNA contamination. The reverse transcription reaction was carried out using High Capacity cDNA Reverse Trenscription Kit (ABI). Quantitative PCR analysis was performed by Step One$^{TM}$ software ve2.0. (ABI) using SYBER Green Master Mix (ABI). Primer sequence for qPCR or PCR were described in supplementary Table II or III, respectively.

***Microarray analysis***

Mouse bone marrow derived dendritic cells were stimulated with polyIC (upper panel) or infected with MV (lower panel) with anti-IFN-AR antibody. Total RNA was extracted from the cells, and we performed microarray analysis using Affimetrix GeneChip Mouse 430.2 (10). The data was analyzed by GeneSpringGX11 software.

***RNA interference***

RNAi vectors were constructed by the insertion of oligonucleotides into *Xba*I/*Pst*I site of the pH1 vector. The target sequence for DDX60 is 5' - CTTTACCACTTTCCTACGA - 3', EXOSC4 is 5' – TATAGTTCAGCGACCTT - 3', EXOSC5 is 5'- GGATCCTACATCCAAGCAA - 3'. 24-well plate HeLa cells or HEK293 cells were transfected with RNAi vector (0.5 μg) using FuGENE HD (Roche), after incubation for 24 h, cells were recovered and suspended to 12 ml medium, then seeded to 24-well plate. 24 h after incubation, puromycine (1.0 μg/ml) was added. The medium containing puromycine was changed every 5 days, puromycine resistant colonies were recovered and the mRNAs of endogenous DDX60 or EXOSC4, EXOSC5 were checked by RT-PCR. The sequences of the primers used for RT-PCR are as described in supplementary table III. siRNA for DDX60 was purchased from Ambion, and was transfected with Lipofectamin 2000 reagent (Invitrogen). The target sequence is 5' – GGC TAA CAA ACT TCG AAA A – 3'

***Immunoprecipitation***

HEK293FT cells were transfected in 6-well plates with plasmids encoding FLAG-tagged RIG-I, MDA5, EXOSC1, EXOSC4, EXOSC5, LGP2, IKK-ε, Ubc13, and/or HA-tagged DDX60. The plasmid amounts were normalized by the addition of empty plasmid. 24 h after transfection, cells were lysed with lysis buffer (20 mM Tris-HCl (pH 7.5), 150 mM NaCl, 1mM EDTA, 10% glycerol, 1% Nonidet P-40, 30 mM NaF, 5 mM $Na_3VO_4$, 20 mM iodoacetamide, and 2 mM phenylmethylsulfonyl fluoride), and then proteins were immunoprecipitated with rabbit anti-HA polyclonal (Sigma) or

anti-FLAG M2 monoclonal antibody (Sigma). The precipitates were analyzed by SDS-PAGE and stained with anti-HA polyclonal or anti-FLAG M2 monoclonal antibody or monoclonal antibody to RIG-I（Alme-1）（ALEXIS BIOCHEMICALS）.

***Confocal Microscopy***

HeLa and HEK293 cells were plated onto micro cover glasses (matsunami) and poly-L-Lysin coated cover glasses (eBioscience), respectively, in a 24-well plate and the following day, cells were transfected with the indicated plasmids. 24 h after transfection, cells were infected with VSV or transfected with polyI:C using 0.5 μg/ml DEAE dextran for 4 h, then fixed using 3% formaldehyde in PBS for 30 min and permeabilized with 0.2% Triton X-100 for 15 min. Fixed cells were blocked in 1% bovine serum albumin in PBS for 10 min and labeled with the indicated primary Abs (5 μg/ml) for 60 min at room temperature. Alexa-conjugated secondary Abs (1:400) were used to visualize staining of the primary Abs for 30 min at room temperature, and mounted onto glass slides using PBS containing 2.3% 1,4-diazabicyclo[2.2.2]octane and 50% glycerol or Prolong Gold Antifade Reagent with DAPI (Invitrogen). Cells were visualized at a magnification of ×63 with an LSM510 META microscope (Zeiss). To stain the mitochondria, ER, early endosome, and autophagosome, we used Mitotracker (Invitrogen), α-calnexin polyclonal antibody (Stressgen), α-EEA1 polyclonal antibody (ABR), and α-LC3 polyclonal antibody (MBL), respectively.

***Reporter Gene Analysis***

HEK293 cells were transiently transfected in 24-well plates using FuGENE HD (Roche) with expression vectors, reporter plasmids, and internal control plasmid coding *Renilla* luciferase. The total amounts of plasmids were normalized with empty vector. For polyI:C stimulation, twenty-four hours after transfection, cells were stimulated with medium containing polyI:C(50 μg/ml) and DEAE-dextran (0.5 μg/ml) for 1h, and then the medium was exchanged with normal medium and incubated for an additional 3h. dsRNA was transfected using Lipofectamine 2000 (Invitrogen). Cells were lysed with lysis buffer (Promega) and luciferase, and *Renilla* luciferase activities were measured by the dual luciferase assay kit (Promega). Relative luciferase activities were calculated by normalizing luciferase activity by control in which only empty vector, reporter, and internal control plasmid were transfected.

***Viruses***

VSV Indiana strain, poliovirus Mahoney strain, HSV-1 K strain, and SeV HVJ strain were amplified using Vero cells. To determine the virus titer, we performed plaque assay using Vero cells. To observe the cytopathic effect, virus infected cells were fixed at indicated time using 10% formaldehyde in PBS for 10 min, then, stained by 1% crystal violet in PBS for 5 min at room temperature.

***DDX60 helicase Recombinant Protein***

DDX60 helicase domain (2254 - 4047 bp) was amplified by PCR using primers DDX60 helicase-F and DDX60 helicase-R. The obtained cDNA fragment was cloned into

*Kpn*I/*Sal*I restriction sites of pCold II DNA vector. The primers sequences are as follows. DDX60 helicase-F, CGGGGTACCATGAGAAAAGACCCAGATCCCAG and DDX60 helicase-R GACGCGTCGACTTTTCCTATTTTGGGGAATG. DDX6 helicase domain (114-429aa) was amplified by RT-PCR using primers F: GGC GGG GTA CCA TGG GCT GGG AAA AGC CAT C and R: GGA CGC GTC GAC ACC AAA GCG ACC TGA TCT TC. The cDNA fragment was cloned into the *Kpn*I/*Sal*1 sites of pCold II DNA vector. Expression vectors were introduced into *E. coli* BL21 competent cells and cultured in 10 ml of ampicillin added LB medium for 12 h at 37 ℃, then added it to 250 ml LB medium and cultured for 3 h at 37 ℃. The cells were incubated at 15 ℃ for 30 min, and protein expression was induced by the addition of 1 mM IPTG. The cells were then cultured at 15 ℃ for 24 h. The culture fluid was centrifuged 10 min, 10,000 rpm, 4 ℃, and recovered the *E.coli*. Suspended 5 mL of Tag binding buffer (20 mM Tris-HCl (pH 7.4), 0.5 M NaCl, 20 mM imidazol, 10% Glycerol), and added 5 mg lysozyme for 30 min on ice, shaking for 10 min, then added 10% Triton X-100 500 μL, incubated for 10 min, centrifuged 30 min 5,000 rpm. The reaction was conducted at 4℃. The supernatant was filtrated using 0.45 μm filter. The protein was purified with His trap HP (GE healthcare) in accordance with the manufacturer's protocol. The protein was eluted with elution buffer (20 mM Tris-HCl (pH7.4), 0.5 mM NaCl, 200 mM imidazol, 10% Glycerol). Collected non-absorbed fraction (sample dropped out after applied to the column), wash fraction (sample dropped out after washing by binding buffer), 500 μl of 10 elute fraction. The obtained samples were checked its purification by SDS-PAGE, detected by CBB.

***RNA synthesis***

VSV-G RNA was synthesized from plasmid by using Riboprobe combination system SP6/T7 RNA polymerase (Promega) in accordance with the manufacturer's protocol. VSV RNA was produced from PCR products, VSV G-pGEM-T Easy for its template and amplified by using 5' primer containing the T7 promoter (TAATACGACTCACTATAGGG) and 3' primer containing the SP6 promoter (GATTTAGGTGACACTATAG). The dsRNA was made by mixing equal amount of +strand (SP6) and –strand (T7). The obtained ss or dsRNA was added DNaseI (Promega) 10 U 37 ℃ for 30 min and purified by phenol/chroloform treatment.

***Gel shift assay***

The final concentration of the reaction solution was BSA 0.02 mg/ml, $MgCl_2$ 10 mM, DTT 0.1mM, glycerol 20%, NaCl 200 mM, Tris-HCl 20 mM and ssRNA 0.6 μg, dsRNA 0.24 μg, or dsDNA 0.1 μg then added DDX60 or DDX6 helicase recombinant protein. The total volume was fixed to 20 μl by adding water. The reaction solution was Incubated 30℃ for 30 min, then 1% agarose gel electrophoresis 4 ℃ for 90 min and observed the RNA by EtBr.

***Pull down assay***

The RNA used for the assay was purchased from JBioS. The RNA sequences are (sense strand) AAA CUG AAA GGG AGA AGU GAA AGU G, (antisense strand) CAC UUU

CAC UUC UCC CUU UCA GUU U. The biotin is conjugated at U residue at the 3' end of antisence strand (underlined). Biotinylated dsRNA were phosphorylated by T4 polynucleotide kinase (TAKARA). dsRNA was incubated for 1hr at 25 $^{o}$C with 10 μg of protein from the cytoplasmic fraction of cells that were transfected with Flag-tagged RIG-I and/or HA-tagged DDX60 expressing vectors. The mixture was transferred into 400 μl of lysis buffer (20 mM Tris-HCl (pH 7.5), 150 mM NaCl, 1 mM EDTA, 10 % Glycerol, 1 % NP-40, 30 mM NaF, 5mM $Na_3VO_4$, 20 mM iodoacetamide, and 2mM PMSF) containing 25 μl of streptavidine Sepharose beads, rocked at 4 $^{o}$C for 2 h, collected by centrifugation, washed three times with lysis buffer, resuspended in SDS sample buffer.

## RESULTS

### *Phylogenetic analysis of the DExD/H box domain of DDX60*

The DDX60 protein contains a DExD/H box RNA helicase domain and a long N- and C-terminal regions with no typical domains or motifs (Fig. 1A). The DExD/H box domain is common with the human genome. Phylogenetic analysis using amino acid sequences from this domain revealed that DDX60 is clustered within a group including RIG-I, MDA5, DICER1, and SKIV2L (bootstrap probability, 93%.), and is most closely related to SKIV2L (bootstrap probability, 90%) (Fig. 1B). The functions of RIG-I and MDA5 have been described above. Dicer is an evolutionarily conserved protein required for RNAi and is known to perform antiviral functions in *D. melanogaster* (12, 48, 51). SKIV2L is a homolog of *S. cerevisiae* Ski2, an antiviral protein that acts

against dsRNA virus. Thus, the DDX60 DExD/H box domain is found to cluster into a group composed of evolutionarily conserved antiviral helicases.

***Expression of DDX60 mRNA***

We carried out the microarray analysis using mouse bone-marrow derived dendritic-cells (BM-DCs), and found that RLRs and DDX60 were included in the helicases whose expressions were increased over four-fold in response to viral infection (Fig. 2A and B). We investigated the expression profile of human DDX60 mRNA by northern blot analysis, and detected a single mRNA band at approximately 5.5 kb position in the human brain, lymph node, prostate, stomach, thyroid, tongue, trachea, uterus, skeletal muscle, spleen, kidney, liver, and small intestine (Fig. 2C). Next, we examined the regulation of DDX60 expression. DDX60 mRNA was detected in unstimulated cells, such as mouse BM-DCs, HeLa, HEK293, and Raw264.7 cells (Fig. 2, D-F). DDX60 expression was up-regulated by stimulation with polyI:C (Fig. 2D) or IFN-β (Fig. 2E). However, DDX60 expression was not increased by TNF-α or IL-1β stimulation (Fig. 2E). Interestingly, DDX60 mRNA was increased by infection with VSV (Fig. 2F) or PV (Fig. 2, G and H). Thus, DDX60 is an interferon-inducible gene, and is upregulated during VSV or PV infection.

***DDX60 associates with the components of the RNA exosome***

Since the sequence of DDX60 is similar to that of the RNA exosome cofactor SKIV2L, we examined whether the DDX60 protein associates with the RNA exosome core

components in the same manner as the cofactor proteins. The RNA exosome core components form a tight protein complex (18), and thus, it is expected that one of the core components will be co-immunoprecipitated with other core components and cofactors of the RNA exosome. These core components include the EXOSC1 and 4. DDX60 protein was observed to co-immunoprecipitate with EXOSC1 and EXOSC4 (Fig. 3, A and B), indicating the physical interaction of DDX60 with EXOSC1 and 4. We used partial DDX60 fragments to identify the region of DDX60 that binds to RNA exosome. EXOSC4 was co-immunoprecipitated with the N-terminal 169 aa fragment of DDX60, indicating that the RNA exosome binds to the N-terminal region of DDX60 (Fig. 3C). All fragments were localized in the cytoplasmic region (Fig. 3D).

***Intracellular localization of DDX60***

Next, we studied the intracellular localization of the DDX60 protein using confocal microscopy. In resting cells, DDX60 was localized in the cytoplasmic region but not in the nucleus before and after polyI:C stimulation or viral infection (Fig. 4, A and B). EXOSC1, 4, and 5 were localized at both cytoplasm and nucleus. The DDX60 protein was partially co-localized with the RNA exosome components at cytoplasmic region (Fig. 4, C-E). To observe the intracellular localization of DDX60 after viral infection, we used HEK293 cell clones stably expressing HA-tagged DDX60. Most DDX60 staining was not colocalized with mitochondria, endoplasmic reticulum (ER), LC3 (autophagosome marker), and endosome markers (EEA1) (Fig. 4, F-I). However, the DDX60-HA protein was partially co-localized with ER after VSV infection (Fig. 4F)

and mitochondria after SeV infection (Fig. 4G).

***Antiviral activity of DDX60 is independent of the RNA exosome***

DDX60 expression was found to increase after viral infection, and RNA exosome plays an antiviral role in lower eukaryote such as budding yeast. Therefore, we assessed the antiviral activity of both DDX60 and the RNA exosome. In our experimental condition, 70 % - 90 % of cells expressed the proteins encoded by the transfected plasmids. Overexpression of three core components (EXOSC1, 4, and 5) suppressed the CPE (Fig. 5A) and reduced the viral titer in case of low MOI (0.1) (Fig. 5B). Next, we performed an shRNA knockdown assay. We used shRNAs for EXOSC4 and EXOSC5, which was previously described to efficiently reduce the expression of the target mRNA (4). We confirmed that shRNAs for EXOSC4 and 5 effectively reduced the expression of their target mRNAs and the proteins (Fig. 5C). Partial decrease of EXOSC4 by knockdown is known to reduce the cell growth (47). We observed that shRNA for EXOSC4 and 5 reduced the cell growth (Fig. 5D), however knockdown of EXOSC4 or 5 showed marginal effect on VSV replication (Fig. 5E) at least in our experimental condition. We do not exclude the possibility that knockdown of EXOSC4 or 5 are not efficient to reduce antivirus role of RNA exosome. Unexpectedly, the physical interaction between EXOSC4 and DDX60 was reduced after VSV infection (Fig 5F).

We next examined the antiviral activity of DDX60. Interestingly, DDX60 overexpression suppressed the CPE by VSV infection, and reduced VSV replication in HEK293 and HeLa cells (Fig. 6, A-D). The suppression by DDX60 overexpression was

observed even in EXOSC5 knockdown cells (Fig. 6B). PV replication was also suppressed by overexpression of DDX60 (Fig. 6E). Next, we performed a knockdown assay using shRNA for DDX60, which reduced the expression of DDX60 mRNA and protein (Fig. 6F, Fig. 11, D, H, L, and Fig. 12G). Unlike EXOSC4 and 5, knockdown of DDX60 increased VSV replication and enhanced CPE, and did not inhibit the cell growth (Fig. 5D and Fig. 6, G and H). Because the interaction between DDX60 and the RNA exosome core component was reduced after viral infection, we examined the molecular mechanism of how DDX60 suppresses viral replication.

***DDX60 associates with RIG-I-like receptors***

To identify the antiviral pathway, in which DDX60 is involved, we used immunoprecipitation assay to search for the protein that binds to DDX60. Because the RLR-dependent pathway plays an important role in the antiviral activity of the host cell, we examined the binding of DDX60 to proteins involved in this pathway. Interestingly, DDX60 was co-immunoprecipitated with RIG-I, MDA5, and LGP2, but not with IPS-1 or IKK-ε, which are downstream factors of RIG-I and MDA5 (Fig. 7A). RNase A or RNase III treatment did not abolish the interaction between DDX60 and RIG-I or MDA5 (Fig. 7, B and C), indicating that these associations are not mediated via RNA. DDX60 did not bind to HMGB1 before or after dsRNA stimulation or VSV infection (Fig. 7D). To further confirm the binding of DDX60 to RIG-I, we examined the interaction of DDX60 with the endogenous RIG-I using anti-RIG-I monoclonal antibody. RIG-I mRNA is known to increase after viral infection (59). We observed an

increase of RIG-I protein after poly I:C stimulation (data not shown). However, the protein level in HEK293FT cells was not increased after VSV infection in our experiment due to unknown reasons (Fig. 7E). Endogenous RIG-I was found to interact with DDX60 after VSV infection but not in its absence (Fig. 7E), indicating that interaction between DDX60 and endogenous RIG-I is dependent on viral infection, although the interaction between overexpressed RIG-I and DDX60 was independent of viral infection.

Next, we used confocal microscopy to examine the intracellular colocalization of DDX60 with RIG-I and MDA5. Consistent with the immunoprecipitation assay, confocal microscopic analysis showed that DDX60 was partially colocalized with overexpressed RIG-I and MDA5 before and after VSV infection or polyI:C stimulation (Fig. 7, F and G). We tried to observe endogenous RIG-I by confocal microscope, however we could not detect endogenous RIG-I by technical reason as far as we tested. We also used RIG-I partial fragments to identify the region of RIG-I that binds to DDX60 (Fig. 7H). RIG-IC, which includes a helicase domain and CTD, was co-immunoprecipitated with DDX60, while the N-terminal CARD of RIG-I was not (Fig. 7H). These data indicate that DDX60 binds to the RIG-IC fragment.

***The DDX60 helicase domain binds to viral RNA***

In light of the binding of DDX60 to viral RNA sensors RIG-I and MDA5, we hypothesized that the RNA helicase domain of DDX60 binds to viral RNA. To test this hypothesis, we expressed a histidine-tagged DDX60 RNA helicase domain (752 – 1337

aa) in *Escherichia. coli* (Fig. 8A). The protein was purified using Ni-NTA resin, analyzed by SDS-PAGE, and stained with CBB. Protein purity was found to be greater than 90% (Fig. 8B). VSV single- and double-stranded RNA was synthesized *in vitro*. Binding of the DDX60 helicase domain to *in vitro*-synthesized viral RNA was examined using gel-shift assay. Single- or double-stranded VSV RNA mobility was found to decrease by the addition of DDX60 helicase (Fig. 8, C and D). DDX60 was also found to bind to dsRNA treated with alkaline phosphatase, suggesting that the presence of 5' triphosphate is nonessential for this binding (Fig. 8E). The mobility shift of ssRNA was different from that of dsRNA, this difference might be caused due to stoichiometry. Interestingly, dsDNA was also shifted in the presence of DDX60 protein (Fig. 8F). As a control we used DDX6, a DExD/H box RNA helicase distantly related to DDX60. DDX6 also bound to ssRNA (Fig. 8C), however DDX6 hardly reduced the mobility of dsRNA and dsDNA compared to DDX60 (Fig. 8D and F).

***DDX60 promotes RIG-I- or MDA5-dependent expression of type I IFN***

Next, we examined whether DDX60 is involved in RIG-I- or MDA5-mediated signaling. The prepared polyI:C solution contains various lengths of polyI:C, both shorter and longer than 1 kbp (data not shown), in a mixture known to activate both RIG-I and MDA5 (20). Both RIG-I-mediated and MDA5-mediated IFN-β promoter activation by polyI:C transfection were enhanced by DDX60 expression (Fig. 9, A and B). As a control we used DDX6, a helicase distantly related to DDX60. Expression of DDX6 produced neither a positive nor a negative effect on the RIG-I-dependent IFN-β

promoter activation (Fig. 9C). To address the function of DDX60 helicase domain, we introduced the mutation (K791A) on the Walker type ATP binding site, which is essential for ATPase activity of RNA helicase (50). The mutation reduced the enhancement of RIG-I-mediated IFN-β promoter activation by DDX60 (Fig. 9C). Knockdown analysis using shRNA for DDX60 showed that IFN-β promoter activation by viral dsRNA was reduced in DDX60 knockdown cells compared with control cells (Fig. 9D). To exclude the off-target effect, we also used siRNA for DDX60, whose target sequence is different from that of shRNA for DDX60. The expression of DDX60 was efficiently reduced by siRNA for DDX60, and the siRNA for DDX60 efficiently reduced the IFN-β mRNA expression by polyI:C stimulation (Fig. 9, E-G). These knockdown results are consistent with the overexpression results described above, providing further evidence that DDX60 promotes the RLR-mediated IFN-β expression.

In contrast, TICAM-1- and TLR3-mediated IFN-β promoter activation were not increased by overexpression of DDX60 (Fig. 9, H and I). In addition, poly I:C stimulation of TLR3 without transfection resulted in normal expression of IFN-β in DDX60 knockdown cells (Fig. 9J). These data suggest that DDX60 is specific to the RLR pathway. Because the knockdown of EXOSC4 or 5 did not reduce the promoter activation resulting from VSV infection or dsRNA transfection (Fig. 9, K and L), the data suggests that these proteins do not play a major role in DDX60-mediated enhancement of RIG-I or MDA5 signaling at least in our experimental condition. We also assessed the effect of DDX60 knockdown on IFN-β promoter activation by overexpressing TBK1, IPS-1, RIG-I CARDs, or MDA5 to find out the step, at which

DDX60 plays a role in RIG-I-mediated signaling. All these lead to the autoactivation, inducing the transcription from the IFN-β promoter in the absence of RIG-I or MDA5 ligands (22). Although DDX60 knockdown reduces the IFN-β promoter activation induced by dsRNA transfection, it was not found to affect this autoactivation (Fig. 9, M and N). These data suggest that shRNA suppression of DDX60 occurs upstream of RIG-I and MDA5 (Fig. 9O).

To examine the effect of DDX60 on the binding of RIG-I to dsRNA, we performed pull down assay. The proteins were exogenously expressed in HEK293FT cells, and the proteins were recovered from cell lysates using biotin-conjugated dsRNA and streptoavidine Sepharose. RIG-I or DDX60 protein was recovered from cell extract, suggesting the binding of RIG-I or DDX60 to dsRNA. Because both RIG-I and DDX60 can bind to dsRNA, the data does not mean the interaction between RIG-I and DDX60. Interestingly, co-expression of both proteins increased the proteins recovered from cell lysate (Fig. 10).

***DDX60 is important for the expression of type I IFN and IFN inducible genes during viral infection***

We next tested whether DDX60 is involved in cytokine expressions during viral infection. RIG-I recognizes VSV and SeV, and MDA5 recognizes PV (3, 21). Interestingly, knockdown of DDX60 reduced IFN-β expression in HeLa cell after VSV, PV, and SeV infection. IFIT-1 and IP10 expression after VSV and SeV infection were also reduced by DDX60 knockdown (Fig. 11). Knockdown of DDX60 caused marginal

effect on the expression of IFIT1 and IP10 in response to PV infection. Some of IFN-α gene expressions induced by other sensor molecules might cause the difference. Unlike viral infection, knockdown of DDX60 did not reduce the expression of IFIT1 after IFN-β stimulation (Fig. 12A). Reduction of type I IFN expression was also observed after VSV infection in HEK293 cells (Fig. 12, B and C). In addition, DDX60 knockdown reduced IRF-3 dimerization after VSV infection (Fig. 12D). These data indicate that DDX60 is required for RIG-I- and MDA5-dependent type I IFN and IFN-inducible gene expression during viral infection. We also observed that the suppression of CPE and viral titer in culture medium by DDX60 overexpression can be reduced by IPS-1 knockdown (Fig. 6, I and J), confirming that the antiviral activity of DDX60 is dependent on RLRs. Because the DDX60 helicase domain was found to bind to dsDNA, we examined whether DDX60 is involved in type I IFN expression after infection with DNA virus HSV-1. In this case, knockdown of DDX60 reduced the expression of IFN-β and IP10 after HSV-1 infection (Fig. 12, E and F).

## DISCUSSION

Here, we report that DDX60 is a novel antiviral factor in human cells. The amino acids sequence of DDX60 is similar to that of Ski2 homologs, which are cofactors of the RNA exosome. DDX60 interacts with core components of the RNA exosome. After viral infection, the DDX60 protein binds to endogenous RIG-I protein, and is involved in RIG-I-dependent pathway. The protein also binds to MDA5 and LGP2. The DDX60 helicase domain binds to viral RNA and DNA, and the co-expression of RIG-I with

DDX60 increases the binding of RIG-I and DDX60 to dsRNA. Knockdown of DDX60 reduces the expression of type I IFN and IFN inducible gene after VSV, PV, SeV, and HSV-1 infections. Therefore, we concluded that DDX60 is a novel antiviral helicase involved in RLR-dependent pathways.

Schroder et al. and Soulat et al. firstly described that non-RLR helicase, DDX3, plays pivotal roles in RLR-dependent pathway (41, 43). DDX3 is ubiquitously expressed in a variety of cells, and exerts its positive effect as a part of TBK-1- and/or IKK-ε-containing complex that activate IRF-3 (41). DDX3 also binds to RIG-I and IPS-1, and promotes the activation of those proteins (28, 32). Our study shows that another non-RLR helicase, DDX60, is also involved in RLR-dependent pathway. Thus, our reports with previous studies demonstrate the important roles of non-RLR helicases in RLR-mediates signaling and antiviral response.

Because DDX60 protein does not contain CARDs, which are required for the interaction with IPS-1, it seems unlikely that DDX60 directly activates IPS-1 without RLRs. Knockdown studies suggest that DDX60 is an upstream factor of IPS-1, and the immunoprecipitation assay results suggest that DDX60 binds to the upstream factors, RLRs. Based on these findings, we expected that DDX60 would bind to viral RNA. The gel shift assay shows that DDX60 helicase can bind to dsRNA, and the pull down assay showed that co-expression of DDX60 with RIG-I increased the binding of RIG-I to dsRNA. Thus, we speculate that DDX60 binds to viral dsRNA and associates with RLRs during viral infection. Further study is required to reveal the precise molecular mechanism of how DDX60 activates the RLRs-dependent pathway.

The DDX60 helicase domain binds to dsDNA *in vitro*, and DDX60 was required for type I IFN expression during infection with the DNA virus, HSV-1. In human cells, RIG-I is involved in the pathway activated by cytoplasmic B-DNA or DNA virus infection (1, 6, 7). A-T rich dsDNA is transcribed by RNA polymerase III, and these transcripts are recognized by RIG-I (1, 6). In contrast, Choi *et al* reported that the RIG-I protein associates with B-DNA and activates the signaling. Previously, Takahasi et al. reported that purified RIG-I protein does not itself bind to dsDNA (46). Therefore, RIG-I seems to associate with B-DNA via another protein that directly binds to dsDNA. HSV-1 was reported to produce considerably amounts of dsRNA and to activate RIG-I and MDA5 (25, 34, 52). Thus, we do not exclude the possibility that DDX60 is involved in recognition of not dsDNA but dsRNA derived from HSV-1. Although RIG-I and MDA5 are involved in the signaling induced by cytoplasmic B-DNA, IPS-1 is dispensable for the signaling (23). Further study is required to reveal the molecular mechanism of how DDX60 plays an important role in the singling induced by cytoplasmic B-DNA.

In addition to *DDX60*, the human genome includes the closely related *DDX60L* gene, which is located 5' upstream of *DDX60* on chromosome IV. However, the mouse genome encodes only one DDX60 protein. Our phylogenetic analysis indicated that the mouse gene is a common ancestor of human *DDX60* and *DDX60L* genes, and a pilot study has revealed that DDX60L is expressed after viral infection (unpublished results). Therefore, DDX60L is also expected to be an antiviral protein. Considering that knockdown of DDX60 severely reduced type I IFN expression after viral infection,

there seems to be functional differences between DDX60 and 60L. Further study is required to reveal the functional differences between DDX60 and 60L.

The amino acid sequence of DDX60 is weakly similar to that of exosome cofactors, SKIV2L or SKIV2L2. In immunoprecipitation experiments, DDX60 protein was found to co-immunoprecipitate with core components of the RNA exosome. However, we could not reveal the physiological role of the interaction between DDX60 and RNA exosome by knockdown analysis. We have examined whether knockdown of DDX60 and RNA exosome delays the degradation of viral genomic RNA or not. We have found that knockdown of DDX60 or RNA exosome components does not substantially delay the degradation of transfected viral RNA (unpublished results). This observation is consistent with our results that knockdown of the RNA exosome does not increase viral titer. However, we do not exclude the possibility that RNA exosome is involved in antiviral responses. There exist several antiviral nucleases, such as RNaseL and ISG20. Thus it is possible that those antiviral nucleases might compensate the defect of RNA exosome. This possibility is not surprising, because there are several redundant pathways in innate immune system. For example, poly IC is a common ligand of TLR3 and MDA5, and thus not single but double knockout is required to abolish the polyI:C-dependent NK cell cytotoxicity (27). Type I IFNs are produced from various kinds of cells, such as fibroblast, dendritic cells, and macrophages, and thus we do not exclude the possibility that the RNA exosome some roles in DDX60 antiviral activity in other cells. The RNA exosome is required to maintain the integrity of host RNA and to disrupt RNA that lacks a 5' CAP or 3' polyA tail. Thus, it is also

possible that DDX60 might be involved in host RNA integrity. Further study is required to reveal the physiological role of the association of DDX60 with RNA exosome.

In single-cell organisms, such as budding yeast (*S. cerevisiae*), Ski2 plays a major role in antiviral response against dsRNA virus. DDX60, a homolog of Ski2, is conserved among eukaryotes. For example, DDX60 is also encoded by the *C. elegans* genome. In a pilot study, we found nematode DDX60 expression to be increased after viral infection (unpublished results), leading us to expect that DDX60 possesses antiviral activity in this species as well. Phylogenetic tree analysis has shown that antiviral helicases, such as DDX60, RLRs, and Dicer, are clustered into one node. Considering that budding yeast uses Ski2 helicase for its antiviral activity, Ski2-DDX60 protein might represents the most primitive antiviral helicase, which has since diverged into several distinct but similar proteins, such as Dicer and RLRs.

## ACKNOWLEDGEMENTS

This work was supported in part by grants-in-aid from the Ministry of Education, Science and Culture of Japan, and Ministry of Health, Labour, and Welfare of Japan, Mitsubushi Foundation, and Akiyama Foundation. We thank Drs. Matsumoto K., Saito H. (National Research Institute for Child Health and Development), and Takaki H. for microarray data.

## REFFERENCES

1. **Ablasser, A., F. Bauernfeind, G. Hartmann, E. Latz, K. A. Fitzgerald, and V. Hornung.** 2009. RIG-I-dependent sensing of poly(dA:dT) through the induction of an RNA polymerase III-transcribed RNA intermediate. Nat Immunol **10:**1065-72.
2. **Akazawa, T., T. Ebihara, M. Okuno, Y. Okuda, M. Shingai, K. Tsujimura, T. Takahashi, M. Ikawa, M. Okabe, N. Inoue, M. Okamoto-Tanaka, H. Ishizaki, J. Miyoshi, M. Matsumoto, and T. Seya.** 2007. Antitumor NK activation induced by the Toll-like receptor 3-TICAM-1 (TRIF) pathway in myeloid dendritic cells. Proc Natl Acad Sci U S A **104:**252-7.
3. **Barral, P. M., J. M. Morrison, J. Drahos, P. Gupta, D. Sarkar, P. B. Fisher, and V. R. Racaniello.** 2007. MDA-5 is cleaved in poliovirus-infected cells. J Virol **81:**3677-84.
4. **Brouwer, R., C. Allmang, R. Raijmakers, Y. van Aarssen, W. V. Egberts, E. Petfalski, W. J. van Venrooij, D. Tollervey, and G. J. Pruijn.** 2001. Three novel components of the human exosome. J Biol Chem **276:**6177-84.
5. **Chen, G., X. Guo, F. Lv, Y. Xu, and G. Gao.** 2008. p72 DEAD box RNA helicase is required for optimal function of the zinc-finger antiviral protein. Proc Natl Acad Sci U S A **105:**4352-7.
6. **Chiu, Y. H., J. B. Macmillan, and Z. J. Chen.** 2009. RNA polymerase III detects cytosolic DNA and induces type I interferons through the RIG-I pathway. Cell **138:**576-91.
7. **Choi, M. K., Z. Wang, T. Ban, H. Yanai, Y. Lu, R. Koshiba, Y. Nakaima, S. Hangai, D. Savitsky, M. Nakasato, H. Negishi, O. Takeuchi, K. Honda, S. Akira, T. Tamura, and T. Taniguchi.** 2009. A selective contribution of the RIG-I-like receptor pathway to type I interferon responses activated by cytosolic DNA. Proc Natl Acad Sci U S A **106:**17870-5.
8. **Cui, S., K. Eisenacher, A. Kirchhofer, K. Brzozka, A. Lammens, K. Lammens, T. Fujita, K. K. Conzelmann, A. Krug, and K. P. Hopfner.** 2008. The C-terminal regulatory domain is the RNA 5'-triphosphate sensor of RIG-I. Mol Cell **29:**169-79.
9. **Dangel, A. W., L. Shen, A. R. Mendoza, L. C. Wu, and C. Y. Yu.** 1995. Human helicase gene SKI2W in the HLA class III region exhibits striking structural similarities to the yeast antiviral gene SKI2 and to the human gene

KIAA0052: emergence of a new gene family. Nucleic Acids Res **23:**2120-6.

10. **Ebihara, T., M. Azuma, H. Oshiumi, J. Kasamatsu, K. Iwabuchi, K. Matsumoto, H. Saito, T. Taniguchi, M. Matsumoto, and T. Seya.** 2010. Identification of a polyI:C-inducible membrane protein that participates in dendritic cell-mediated natural killer cell activation. J Exp Med **207:**2675-87.

11. **Gack, M. U., Y. C. Shin, C. H. Joo, T. Urano, C. Liang, L. Sun, O. Takeuchi, S. Akira, Z. Chen, S. Inoue, and J. U. Jung.** 2007. TRIM25 RING-finger E3 ubiquitin ligase is essential for RIG-I-mediated antiviral activity. Nature **446:**916-920.

12. **Galiana-Arnoux, D., C. Dostert, A. Schneemann, J. A. Hoffmann, and J. L. Imler.** 2006. Essential function in vivo for Dicer-2 in host defense against RNA viruses in drosophila. Nat Immunol **7:**590-7.

13. **Gao, D., Y. K. Yang, R. P. Wang, X. Zhou, F. C. Diao, M. D. Li, Z. H. Zhai, Z. F. Jiang, and D. Y. Chen.** 2009. REUL is a novel E3 ubiquitin ligase and stimulator of retinoic-acid-inducible gene-I. PLoS One **4:**e5760.

14. **Guo, X., J. Ma, J. Sun, and G. Gao.** 2007. The zinc-finger antiviral protein recruits the RNA processing exosome to degrade the target mRNA. Proc Natl Acad Sci U S A **104:**151-6.

15. **Hayakawa, S., S. Shiratori, H. Yamato, T. Kameyama, C. Kitatsuji, F. Kashigi, S. Goto, S. Kameoka, D. Fujikura, T. Yamada, T. Mizutani, M. Kazumata, M. Sato, J. Tanaka, M. Asaka, Y. Ohba, T. Miyazaki, M. Imamura, and A. Takaoka.** 2010. ZAPS is a potent stimulator of signaling mediated by the RNA helicase RIG-I during antiviral responses. Nat Immunol **12:**37-44.

16. **Hornung, V., J. Ellegast, S. Kim, K. Brzozka, A. Jung, H. Kato, H. Poeck, S. Akira, K. K. Conzelmann, M. Schlee, S. Endres, and G. Hartmann.** 2006. 5'-Triphosphate RNA is the ligand for RIG-I. Science **314:**994-7.

17. **Houseley, J., J. LaCava, and D. Tollervey.** 2006. RNA-quality control by the exosome. Nat Rev Mol Cell Biol **7:**529-39.

18. **Houseley, J., and D. Tollervey.** 2009. The many pathways of RNA degradation. Cell **136:**763-76.

19. **Kato, H., S. Sato, M. Yoneyama, M. Yamamoto, S. Uematsu, K. Matsui, T. Tsujimura, K. Takeda, T. Fujita, O. Takeuchi, and S. Akira.** 2005. Cell

type-specific involvement of RIG-I in antiviral response. Immunity **23:**19-28.

20. **Kato, H., O. Takeuchi, E. Mikamo-Satoh, R. Hirai, T. Kawai, K. Matsushita, A. Hiiragi, T. S. Dermody, T. Fujita, and S. Akira.** 2008. Length-dependent recognition of double-stranded ribonucleic acids by retinoic acid-inducible gene-I and melanoma differentiation-associated gene 5. J Exp Med **205:**1601-10.

21. **Kato, H., O. Takeuchi, S. Sato, M. Yoneyama, M. Yamamoto, K. Matsui, S. Uematsu, A. Jung, T. Kawai, K. J. Ishii, O. Yamaguchi, K. Otsu, T. Tsujimura, C. S. Koh, C. Reis e Sousa, Y. Matsuura, T. Fujita, and S. Akira.** 2006. Differential roles of MDA5 and RIG-I helicases in the recognition of RNA viruses. Nature **441:**101-5.

22. **Kawai, T., K. Takahashi, S. Sato, C. Coban, H. Kumar, H. Kato, K. J. Ishii, O. Takeuchi, and S. Akira.** 2005. IPS-1, an adaptor triggering RIG-I- and Mda5-mediated type I interferon induction. Nat Immunol **6:**981-8.

23. **Kumar, H., T. Kawai, H. Kato, S. Sato, K. Takahashi, C. Coban, M. Yamamoto, S. Uematsu, K. J. Ishii, O. Takeuchi, and S. Akira.** 2006. Essential role of IPS-1 in innate immune responses against RNA viruses. J Exp Med **203:**1795-803.

24. **Li, X., C. T. Ranjith-Kumar, M. T. Brooks, S. Dharmaiah, A. B. Herr, C. Kao, and P. Li.** 2009. The RIG-I-like receptor LGP2 recognizes the termini of double-stranded RNA. J Biol Chem **284:**13881-91.

25. **Melchjorsen, J., J. Rintahaka, S. Soby, K. A. Horan, A. Poltajainen, L. Ostergaard, S. R. Paludan, and S. Matikainen.** 2010. Early innate recognition of herpes simplex virus in human primary macrophages is mediated via the MDA5/MAVS-dependent and MDA5/MAVS/RNA polymerase III-independent pathways. J Virol **84:**11350-8.

26. **Meylan, E., J. Curran, K. Hofmann, D. Moradpour, M. Binder, R. Bartenschlager, and J. Tschopp.** 2005. Cardif is an adaptor protein in the RIG-I antiviral pathway and is targeted by hepatitis C virus. Nature **437:**1167-72.

27. **Miyake, T., Y. Kumagai, H. Kato, Z. Guo, K. Matsushita, T. Satoh, T. Kawagoe, H. Kumar, M. H. Jang, T. Kawai, T. Tani, O. Takeuchi, and S. Akira.** 2009. Poly I:C-induced activation of NK cells by CD8 alpha+ dendritic

cells via the IPS-1 and TRIF-dependent pathways. J Immunol **183:**2522-8.

28. **Oshiumi, H., M. Ikeda, M. Matsumoto, A. Watanabe, O. Takeuchi, S. Akira, N. Kato, K. Shimotohno, and T. Seya.** 2010. Hepatitis C virus core protein abrogates the DDX3 function that enhances IPS-1-mediated IFN-beta induction. PLoS One **5:**e14258.

29. **Oshiumi, H., M. Matsumoto, K. Funami, T. Akazawa, and T. Seya.** 2003. TICAM-1, an adaptor molecule that participates in Toll-like receptor 3-mediated interferon-beta induction. Nat Immunol **4:**161-7.

30. **Oshiumi, H., M. Matsumoto, S. Hatakeyama, and T. Seya.** 2009. Riplet/RNF135, a RING finger protein, ubiquitinates RIG-I to promote interferon-beta induction during the early phase of viral infection. J Biol Chem **284:**807-17.

31. **Oshiumi, H., M. Miyashita, N. Inoue, M. Okabe, M. Matsumoto, and T. Seya.** 2010. The ubiquitin ligase Riplet is essential for RIG-I-dependent innate immune responses to RNA virus infection. Cell Host Microbe **8:**496-509.

32. **Oshiumi, H., K. Sakai, M. Matsumoto, and T. Seya.** 2010. DEAD/H BOX 3 (DDX3) helicase binds the RIG-I adaptor IPS-1 to up-regulate IFN-beta inducing potential. Eur J Immunol **AOP:**DOI 10.1002/eji.200940203.

33. **Pippig, D. A., J. C. Hellmuth, S. Cui, A. Kirchhofer, K. Lammens, A. Lammens, A. Schmidt, S. Rothenfusser, and K. P. Hopfner.** 2009. The regulatory domain of the RIG-I family ATPase LGP2 senses double-stranded RNA. Nucleic Acids Res **37:**2014-25.

34. **Rasmussen, S. B., S. B. Jensen, C. Nielsen, E. Quartin, H. Kato, Z. J. Chen, R. H. Silverman, S. Akira, and S. R. Paludan.** 2009. Herpes simplex virus infection is sensed by both Toll-like receptors and retinoic acid-inducible gene-like receptors, which synergize to induce type I interferon production. J Gen Virol **90:**74-8.

35. **Rehwinkel, J., C. P. Tan, D. Goubau, O. Schulz, A. Pichlmair, K. Bier, N. Robb, F. Vreede, W. Barclay, E. Fodor, and E. S. C. Reis.** 2010. RIG-I detects viral genomic RNA during negative-strand RNA virus infection. Cell **140:**397-408.

36. **Saito, T., R. Hirai, Y. M. Loo, D. Owen, C. L. Johnson, S. C. Sinha, S. Akira, T. Fujita, and M. Gale, Jr.** 2007. Regulation of innate antiviral defenses

through a shared repressor domain in RIG-I and LGP2. Proc Natl Acad Sci U S A **104:**582-7.

37. **Saito, T., D. M. Owen, F. Jiang, J. Marcotrigiano, and M. Gale, Jr.** 2008. Innate immunity induced by composition-dependent RIG-I recognition of hepatitis C virus RNA. Nature **454:**523-7.

38. **Satoh, T., H. Kato, Y. Kumagai, M. Yoneyama, S. Sato, K. Matsushita, T. Tsujimura, T. Fujita, S. Akira, and O. Takeuchi.** 2010. LGP2 is a positive regulator of RIG-I- and MDA5-mediated antiviral responses. Proc Natl Acad Sci U S A **AOP:**doi: 10.1073/pnas.0912986107.

39. **Schlee, M., A. Roth, V. Hornung, C. A. Hagmann, V. Wimmenauer, W. Barchet, C. Coch, M. Janke, A. Mihailovic, G. Wardle, S. Juranek, H. Kato, T. Kawai, H. Poeck, K. A. Fitzgerald, O. Takeuchi, S. Akira, T. Tuschl, E. Latz, J. Ludwig, and G. Hartmann.** 2009. Recognition of 5' triphosphate by RIG-I helicase requires short blunt double-stranded RNA as contained in panhandle of negative-strand virus. Immunity **31:**25-34.

40. **Schmidt, A., T. Schwerd, W. Hamm, J. C. Hellmuth, S. Cui, M. Wenzel, F. S. Hoffmann, M. C. Michallet, R. Besch, K. P. Hopfner, S. Endres, and S. Rothenfusser.** 2009. 5'-triphosphate RNA requires base-paired structures to activate antiviral signaling via RIG-I. Proc Natl Acad Sci U S A **106:**12067-72.

41. **Schroder, M., M. Baran, and A. G. Bowie.** 2008. Viral targeting of DEAD box protein 3 reveals its role in TBK1/IKKepsilon-mediated IRF activation. Embo J **27:**2147-57.

42. **Seth, R. B., L. Sun, C. K. Ea, and Z. J. Chen.** 2005. Identification and characterization of MAVS, a mitochondrial antiviral signaling protein that activates NF-kappaB and IRF 3. Cell **122:**669-82.

43. **Soulat, D., T. Burckstummer, S. Westermayer, A. Goncalves, A. Bauch, A. Stefanovic, O. Hantschel, K. L. Bennett, T. Decker, and G. Superti-Furga.** 2008. The DEAD-box helicase DDX3X is a critical component of the TANK-binding kinase 1-dependent innate immune response. Embo J **27:**2135-46.

44. **Sun, Q., L. Sun, H. H. Liu, X. Chen, R. B. Seth, J. Forman, and Z. J. Chen.** 2006. The specific and essential role of MAVS in antiviral innate immune responses. Immunity **24:**633-42.

45. **Takahasi, K., H. Kumeta, N. Tsuduki, R. Narita, T. Shigemoto, R. Hirai, M. Yoneyama, M. Horiuchi, K. Ogura, T. Fujita, and F. Inagaki.** 2009. Solution structures of cytosolic RNA sensor MDA5 and LGP2 C-terminal domains: identification of the RNA recognition loop in RIG-I-like receptors. J Biol Chem **284:**17465-74.

46. **Takahasi, K., M. Yoneyama, T. Nishihori, R. Hirai, H. Kumeta, R. Narita, M. Gale, Jr., F. Inagaki, and T. Fujita.** 2008. Nonself RNA-sensing mechanism of RIG-I helicase and activation of antiviral immune responses. Mol Cell **29:**428-40.

47. **van Dijk, E. L., G. Schilders, and G. J. Pruijn.** 2007. Human cell growth requires a functional cytoplasmic exosome, which is involved in various mRNA decay pathways. Rna **13:**1027-35.

48. **van Rij, R. P., M. C. Saleh, B. Berry, C. Foo, A. Houk, C. Antoniewski, and R. Andino.** 2006. The RNA silencing endonuclease Argonaute 2 mediates specific antiviral immunity in Drosophila melanogaster. Genes Dev **20:**2985-95.

49. **Venkataraman, T., M. Valdes, R. Elsby, S. Kakuta, G. Caceres, S. Saijo, Y. Iwakura, and G. N. Barber.** 2007. Loss of DExD/H box RNA helicase LGP2 manifests disparate antiviral responses. J Immunol **178:**6444-55.

50. **Walker, J. E., M. Saraste, M. J. Runswick, and N. J. Gay.** 1982. Distantly related sequences in the alpha- and beta-subunits of ATP synthase, myosin, kinases and other ATP-requiring enzymes and a common nucleotide binding fold. Embo J **1:**945-51.

51. **Wang, X. H., R. Aliyari, W. X. Li, H. W. Li, K. Kim, R. Carthew, P. Atkinson, and S. W. Ding.** 2006. RNA interference directs innate immunity against viruses in adult Drosophila. Science **312:**452-4.

52. **Weber, F., V. Wagner, S. B. Rasmussen, R. Hartmann, and S. R. Paludan.** 2006. Double-stranded RNA is produced by positive-strand RNA viruses and DNA viruses but not in detectable amounts by negative-strand RNA viruses. J Virol **80:**5059-64.

53. **Wickner, R. B.** 1996. Double-stranded RNA viruses of Saccharomyces cerevisiae. Microbiol Rev **60:**250-65.

54. **Widner, W. R., and R. B. Wickner.** 1993. Evidence that the SKI antiviral system of Saccharomyces cerevisiae acts by blocking expression of viral mRNA.

Mol Cell Biol **13:**4331-41.

55. **Xu, L. G., Y. Y. Wang, K. J. Han, L. Y. Li, Z. Zhai, and H. B. Shu.** 2005. VISA is an adapter protein required for virus-triggered IFN-beta signaling. Mol Cell **19:**727-40.

56. **Yanai, H., T. Ban, Z. Wang, M. K. Choi, T. Kawamura, H. Negishi, M. Nakasato, Y. Lu, S. Hangai, R. Koshiba, D. Savitsky, L. Ronfani, S. Akira, M. E. Bianchi, K. Honda, T. Tamura, T. Kodama, and T. Taniguchi.** 2009. HMGB proteins function as universal sentinels for nucleic-acid-mediated innate immune responses. Nature **462:**99-103.

57. **Yoneyama, M., and T. Fujita.** 2007. RIG-I family RNA helicases: cytoplasmic sensor for antiviral innate immunity. Cytokine Growth Factor Rev **18:**545-51.

58. **Yoneyama, M., M. Kikuchi, K. Matsumoto, T. Imaizumi, M. Miyagishi, K. Taira, E. Foy, Y. M. Loo, M. Gale, Jr., S. Akira, S. Yonehara, A. Kato, and T. Fujita.** 2005. Shared and unique functions of the DExD/H-box helicases RIG-I, MDA5, and LGP2 in antiviral innate immunity. J Immunol **175:**2851-8.

59. **Yoneyama, M., M. Kikuchi, T. Natsukawa, N. Shinobu, T. Imaizumi, M. Miyagishi, K. Taira, S. Akira, and T. Fujita.** 2004. The RNA helicase RIG-I has an essential function in double-stranded RNA-induced innate antiviral responses. Nat Immunol **5:**730-7.

## Figure legends

**Fig. 1 The phylogenetic tree of DExD/H box RNA helicase.**

(A) Schematic diagram of DDX60. DDX60 encodes a peptide of 1712 amino acids (aa) that contains a DExD/H box (760-956 aa) and HELICc (1247-1330 aa).

(B) The phylogenetic tree of DExD/H box RNA heliases. Ce, *C. elegans.* The bootstrap probabilities or genetic distances are shown in red and black, respectively.

**Fig. 2 Expression of DDX60 mRNA.**

(A, B) Mouse BM-DCs were stimulated with polyIC (A) or infected with MV in the presence of anti-IFN-AR antibody (B). Total RNA was extracted from the cells, and microarray analysis was performed. The heat maps in left column show the expression profiles of the genes encoding helicase domain. The heat maps in right column show the genes encoding helicase domain whose expressions are changed over 4-fold.

(C) Northern blot of human DDX60 mRNAs in specified tissues. Northern blots of human tissues were probed with DDX60 cDNA.

(D and E) Mouse BM-DCs, HeLa or Raw264.7 cells were stimulated with 50 μg/ml of polyI:C (D), 800 U/ml of IFN-β (E), 100 U/ml of TNF-α (E), or 1000 U/ml of IL-1β (E). The expressions of DDX60, RIG-I, GAPDH, and β-actin mRNA were examined by RT-PCR.

(F and G) HEK293, Raw264.7 cells or HeLa cells were infected with VSV at MOI = 1 (F) or PV at MOI =0.1 (G). Expressions of DDX60, IFN-β, β-actin, and/or GAPDH were examined by RT-PCR (F) or RT-qPCR (G).

(H) PV was injected i.p. into PVR-transgenic mice susceptible to PV. Tissues RNA extraction was performed before or 3 days after infection, and RT-PCR was carried out on these samples.

**Fig. 3 Interactions between DDX60 and RNA exosome components.**

(A, B) HA-tagged DDX60 and FLAG-tagged EXOSC1 (A) and EXOSC4 (B) expression vector were transfected into HEK293FT cells. After 24 h, cell lysates were prepared and immunoprecipitation was performed with anti-FLAG antibody. The

samples were analyzed by SDS-PAGE, and detected by western blotting using anti-HA or -FLAG antibodies.

(C) HA-tagged DDX60 partial fragments and/or FLAG-tagged EXOSC4 expression vectors were transfected into HEK293FT cells, and immunoprecipitation was carried out as in (A) in the presence of RNase A.

(D) HA-tagged DDX60 fragment-expressing vectors were transfected into HeLa cells. The cells were stained with anti-HA antibody and DAPI, and then observed by confocal microscope.

**Fig. 4 Intracellular localization of DDX60.**

(A, B) HA-tagged DDX60 expression vector was transfected into HeLa cells, and transfected cells were stimulated with 50 μg/ml polyI:C (A) or infected with VSV at MOI = 10 (B). The cells were fixed and stained with anti-HA antibodies and observed using confocal microscopy.

(C-E) HA-tagged DDX60 was transfected into HeLa cells together with FLAG-tagged EXOSC1 (C), 4 (D), or 5 (E). Transfected cells were fixed and stained with anti-HA and anti-FLAG antibodies and observed using confocal microscopy.

(F-I) HEK293 cells stably expressing DDX60-HA was infected with VSV or SeV. DDX60-HA was stained with anti-HA antibody. ER, Mitochondria, early endosome, and autophagosome were stained with calnexin (F), Mitotracker Red (G), anti-EEA1 antibody (H), and anti-LC3 antibody (I).

**Fig. 5 Antiviral activity of RNA exosome.**

(A, B) HeLa cells were transfected with expression vectors containing EXOSC1, 4, and 5, and 24 h later, the transfected cells were infected with VSV at MOI = 1 or 0.5. One day after infection, the cells were fixed and stained with crystal violet (A). Viral titers of culture media after 76 h were measured by the plaque assay (B).

(C) The expressions of EXOSC4 and 5 in HeLa stable clones, which express shRNA for EXOSC4, 5, or GFP, were examined by RT-PCR (upper panel), RT-qPCR (middle panel), and western blotting (lower panel). The amounts of EXOSC4 and 5 cDNA in each samples were normalized by dividing by the amount of GAPDH.

(D and E) Cell growth rates of HeLa stable clones, which express shRNA for EXOSC4, 5, DDX60, or GFP, were determined (D). The cells were infected with VSV at MOI = 0.1 for 48 h, and viral titers of culture media were determined by plaque assay (E).

(F) FLAG-tagged EXOSC4 and HA-tagged DDX60-expressing vectors were transfected into HEK293FT cells. After VSV or mock infection, the immunoprecipitation was performed with anti-HA antibody.

**Fig. 6 Antiviral activity of DDX60.**

(A, B) HeLa cells (A) or the cells stably expressing shRNA for EXOSC5 or GFP (B) were transiently transfected with empty, DDX60-expressing, and/or RIG-I-expressing vectors. After 24 h, cells were infected with VSV at MOI = 0.1 for 30 h. Cells were fixed and stained with crystal violet.

(C, D) HEK293 clones stably expressing DDX60 or RIG-I (C) and HeLa cells

transiently expressing mock or DDX60 (D) were infected with VSV at MOI = 0.1 for 24 h (C) or 48h (D). Viral titers of culture media were measured by plaque assay.

(E) Empty or DDX60-expressing vectors were transfected into HeLa cells, and 24 h after transfection cells were infected with PV at MOI = 0.1 for 26 h. Viral titers of culture media were measured by plaque assay.

(F) DDX60-expressing vector was transfected in HeLa clones stably expressing shRNA for GFP or DDX60, and the protein was observed by western blotting.

(G) Control or DDX60 knockdown cells were infected with VSV at MOI = 0.1 for 12 h, and viral titers of the culture media were measured by the plaque assay.

(H) Control and DDX60 knockdown cells were infected with VSV at the indicated MOI for 12 h. The cells were fixed and stained with crystal violet.

(I, J) Empty or DDX60-expressing vectors were transfected into HeLa cells with negative control siRNA or siRNA for IPS-1. The cells were infected with VSV at MOI = 1. After 24 h, cells were stained with crystal violet (I), and the viral titers of culture media were determined by plaque assay (J).

**Fig. 7 Association of DDX60 with RLRs.**

(A-C) Vectors expressing HA-tagged DDX60 were transfected into HEK293FT cells with FLAG-tagged LGP2, RIG-I, MDA5, IPS-1, IKK-ε, and/or Ubc13, and cell lysates were prepared. The lysates were treated with RNase III (B) or RNase A (C). Immunoprecipitation was carried out with anti-FLAG antibody, and the precipitates (IP) and 10 % of whole cell extract (WCE) were analyzed using SDS-PAGE. Proteins were

stained by western blotting using anti-HA or anti-FLAG antibody.

(D, E) HEK293FT cells were transfected with empty or HA-tagged DDX60-expressing vectors, and cells were stimulated with dsRNA or infected with VSV. Cell lysates were prepared at the indicated times, and immunoprecipitation was performed with anti-HA antibody. The precipitates were analyzed using SDS-PAGE, and western blotting was carried out using anti-HA, anti-HMGB1 (D), and anti-RIG-I antibodies (E).

(F, G) Vectors expressing HA-tagged DDX60, FLAG-tagged RIG-I (F) or MDA5 (G) were transfected into HeLa cells. After 24 h, cells were fixed and stained with anti-HA or anti-FLAG antibody, and then observed using confocal microscopy.

(H) The upper panel shows a schematic diagram of RIG-I partial fragments. The lower panel shows results of an immunoprecipitation assay performed as in (A). DDX60 was found to bind to the RIG-IC region.

**Fig. 8 Binding of the DDX60 helicase domain to viral RNA.**

(A) Schematic diagram showing the helicase region of DDX60 used for the following gel shift assay.

(B) A His-tagged DDX60 helicase fragment was expressed in *E. coli*, and purified using Ni-NTA resin. Purified products were analyzed by SDS-PAGE and stained with CBB. Lane A is the non-absorbed fraction, the lane B is the wash fraction, and lanes 1 – 10 are the eluted fractions. Lane 3 fraction contains DDX60 protein.

(C-F) Purified DDX60 and DDX6 fragments were incubated with *in vitro* synthesized VSV ssRNA (C), dsRNA (D), dsRNA treated with CIAP (E), or dsDNA (F), and the

products were analyzed with agarose gel. The gel was stained with ethidium bromide.

**Fig. 9 DDX60 promotes RIG-I- or MDA5-mediated signaling.**

(A-C) Activation of IFN-β promoter was examined in a reporter gene assay using plasmid p125luc. Vectors expressing RIG-I (A), MDA5 (B), DDX6 (C), and WT or DDX60-K791A (C) were transfected into HEK293 cells together with the reporter plasmid and *Renilla* luciferase plasmid (internal control). After 24 h, the cells were stimulated with or without polyI:C using DEAE-dextran for 4 h. Cell lysates were prepared and luciferase activity was measured.

(D) Control or DDX60 knockdown HEK293 cells were transfected with p125luc reporter, *Renilla* luciferase plasmid and/or *in vitro*-synthesized VSV dsRNA. After 24 h, cell lysates were prepared and luciferase activity was measured.

(E and F) siRNA for DDX60 or control siRNA was transfected into HEK293 cells. The cells were stimulated with or without polyI:C, and the expressions of IFN-β and DDX60 mRNA were measured by RT-qPCR. The expressions were normalized by GAPDH.

(G) siRNA for DDX60 or control was transfected into HEK293 cells together with DDX60-expressing vector. The DDX60 protein was observed by western blotting.

(H) Vectors expressing TICAM-1 and/or DDX60 were transfected into HEK293 cells together with p125luc reporter and *Renilla* luciferase plasmids. After 24 h, the cell lysates were prepared and luciferase activities were measured.

(I) Vectors expressing TLR3 and/or DDX60 were transfected into HEK293 cells together with p125luc reporter and *Renilla* luciferase plasmids. After 24 h, the cells

were stimulated with or without polyI:C for 4 h and the cell lysates were prepared and luciferase activity was measured.

(J and K) HeLa cells expressing shRNA for DDX60 (J) or EXOSC4 (K) were stimulated with 50μg/ml of polyI:C (no transfection) (J) or dsRNA (transfection) (K). RT-qPCR was perfomed to measure the expression of IFN-β mRNA expression.

(L) HeLa cells expressing shRNA for GFP, EXOSC4, or EXOSC5 were infected with VSV at MOI = 1. Fold induction of IFN-β mRNA was calculated as in (J).

(M and N) Empty, IPS-1 (M), RIG-I CARD-, MDA5-, or TBK1-expressing vectors (N) were transfected into control or DDX60 knockdown HEK293 cells together with p125luc reporter and *Renilla* luciferase plasmids. After 24 h, cell lysates were prepared and then the luciferase activity was measured.

(O) shRNA for DDX60 did not inhibit the signaling from TLR3 (H-J). Although DDX60 promotes the RLRs-dependent signaling (A-E), shRNA for DDX60 did not reduce the signaling induced by RIG-I CARD, MDA5, IPS-1, or TBK1 overexpression (M and N). These data suggest that shRNA suppresses signaling upstream of RIG-I and MDA5.

**Fig. 10 DDX60 increases the association of RIG-I to short synthetic dsRNA.**

DDX60 and RIG-I expressing vectors were transfected into HEK293FT cells. Twenty-four hours later, the cell lysate were prepared. The lysate was incubated with or without biotin-conjugated dsRNA and the dsRNA was recovered using streptoavidine sepharose beads. The recovered fraction was analyzed by western blotting.

**Fig. 11 Knockdown of DDX60 decreases the expression of type I IFN during viral infection in HeLa cell.**

(A-L) Control or HeLa stable cell line expressing shRNA for DDX60 were infected with VSV (A-D), PV (E-H), or SeV (I-L). Total RNA was extracted at the indicated times. RT-qPCR was performed to measure expression of IFN-β (A, E, and I), IFIT1 (B, F, and J), IP10 (C, G, and K), and DDX60 (D, H, and L). The expression level of each sample was normalized by GAPDH expression.

**Fig. 12 Effects of DDX60 knockdown on antiviral responses.**

(A-C) Control or DDX60 knockdown cells were stimulated with IFN-β (A) or infected with VSV at MOI =1 (B) or 0.1 (C), and the expressions of IFIT1 (A) and IFN-β (B and C) mRNA were examined by RT-qPCR.

(D) Control or DDX60 knockdown HEK293 cells were infected with VSV at MOI = 1, and cell lysates were prepared at the indicated times. Lysates were analyzed by native-PAGE, and western blot was performed with anti-IRF-3 antibody.

(E-G) Control or DDX60 knockdown HeLa cells were infected with HSV-1, and total RNA was extracted at the indicated times. RT-qPCR was performed to examine the expression of IFN-β (E), IP10 (F), and DDX60 (G)

Figure 1

(A)

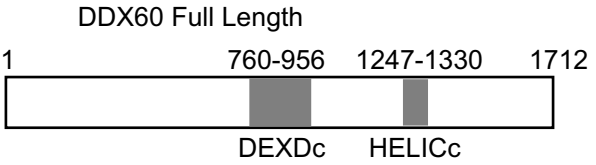
DDX60 Full Length
1
760-956
1247-1330
1712
DEXDc
HELICc

(B)

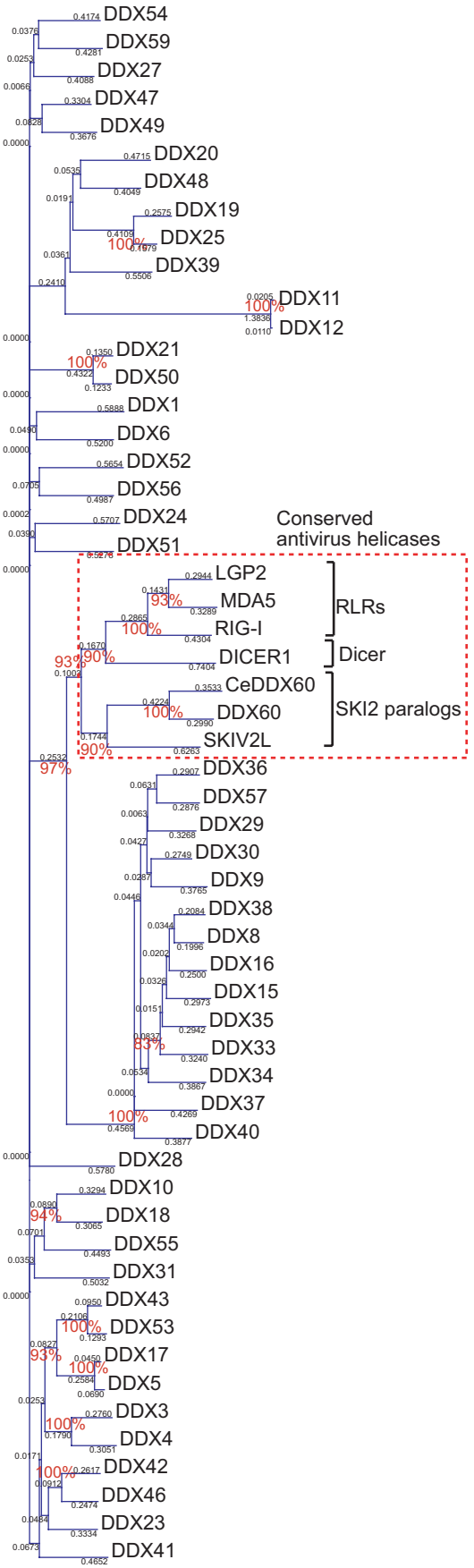
DDX54
DDX59
DDX27
DDX47
DDX49
DDX20
DDX48
DDX19
DDX25
DDX39
DDX11
DDX12
DDX21
DDX50
DDX1
DDX6
DDX52
DDX56
DDX24
DDX51
Conserved antivirus helicases
LGP2
MDA5
RIG-I
RLRs
DICER1
Dicer
CeDDX60
DDX60
SKIV2L
SKI2 paralogs
DDX36
DDX57
DDX29
DDX30
DDX9
DDX38
DDX8
DDX16
DDX15
DDX35
DDX33
DDX34
DDX37
DDX40
DDX28
DDX10
DDX18
DDX55
DDX31
DDX43
DDX53
DDX17
DDX5
DDX3
DDX4
DDX42
DDX46
DDX23
DDX41

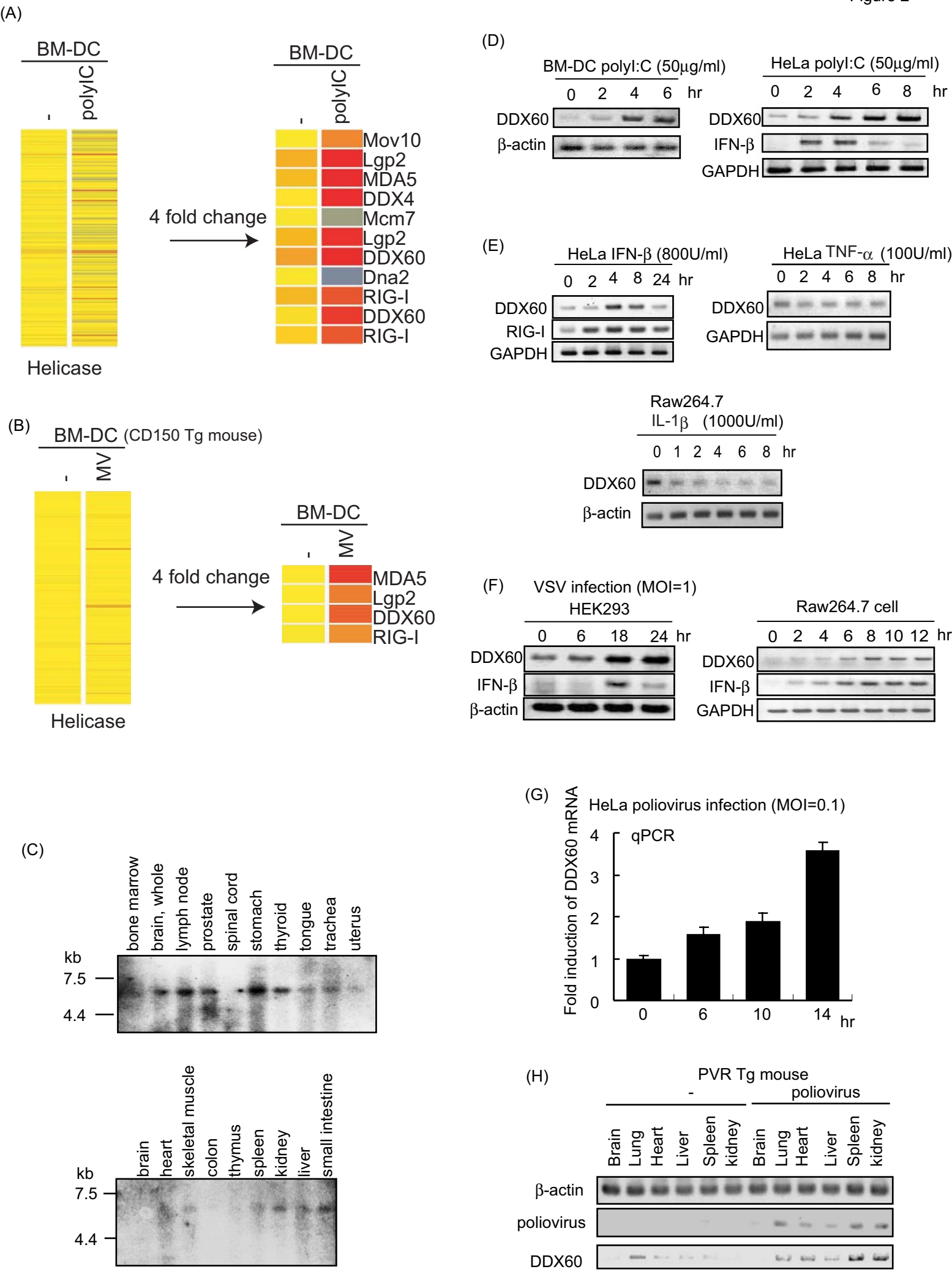
(A)
BM-DC
-
polyIC
4 fold change
Mov10
Lgp2
MDA5
DDX4
Mcm7
Lgp2
DDX60
Dna2
RIG-I
DDX60
RIG-I
Helicase
(B)
BM-DC (CD150 Tg mouse)
-
MV
4 fold change
MDA5
Lgp2
DDX60
RIG-I
Helicase
(C)
bone marrow
brain, whole
lymph node
prostate
spinal cord
stomach
thyroid
tongue
trachea
uterus
kb
7.5
4.4
brain
heart
skeletal muscle
colon
thymus
spleen
kidney
liver
small intestine
kb
7.5
4.4
(D)
BM-DC polyI:C (50μg/ml)
0 2 4 6 hr
DDX60
β-actin
HeLa polyI:C (50μg/ml)
0 2 4 6 8 hr
DDX60
IFN-β
GAPDH
(E)
HeLa IFN-β (800U/ml)
0 2 4 8 24 hr
DDX60
RIG-I
GAPDH
HeLa TNF-α (100U/ml)
0 2 4 6 8 hr
DDX60
GAPDH
Raw264.7
IL-1β (1000U/ml)
0 1 2 4 6 8 hr
DDX60
β-actin
(F)
VSV infection (MOI=1)
HEK293
0 6 18 24 hr
DDX60
IFN-β
β-actin
Raw264.7 cell
0 2 4 6 8 10 12 hr
DDX60
IFN-β
GAPDH
(G)
HeLa poliovirus infection (MOI=0.1)
qPCR
Fold induction of DDX60 mRNA
4
3
2
1
0
0 6 10 14 hr
(H)
PVR Tg mouse
-
poliovirus
Brain
Lung
Heart
Liver
Spleen
kidney
Brain
Lung
Heart
Liver
Spleen
kidney
β-actin
poliovirus
DDX60

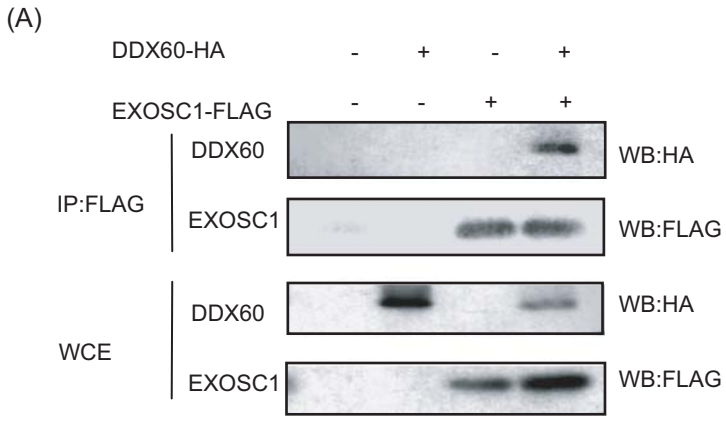
(A)
DDX60-HA - + - +
EXOSC1-FLAG - - + +
IP:FLAG
DDX60
EXOSC1
WB:HA
WB:FLAG
WCE
DDX60
EXOSC1
WB:HA
WB:FLAG

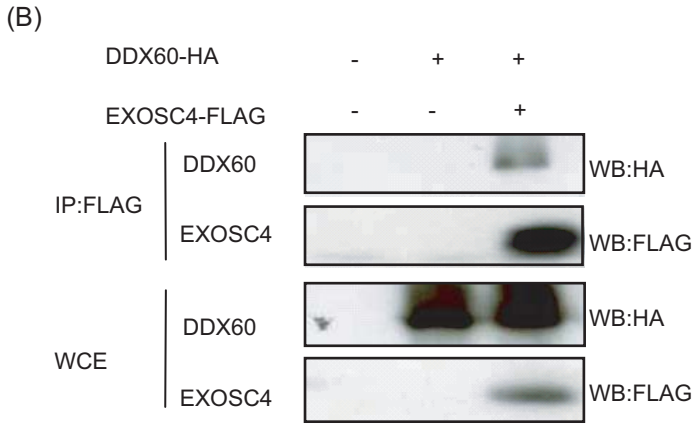
(B)
DDX60-HA - + +
EXOSC4-FLAG - - +
IP:FLAG
DDX60
EXOSC4
WB:HA
WB:FLAG
WCE
DDX60
EXOSC4
WB:HA
WB:FLAG

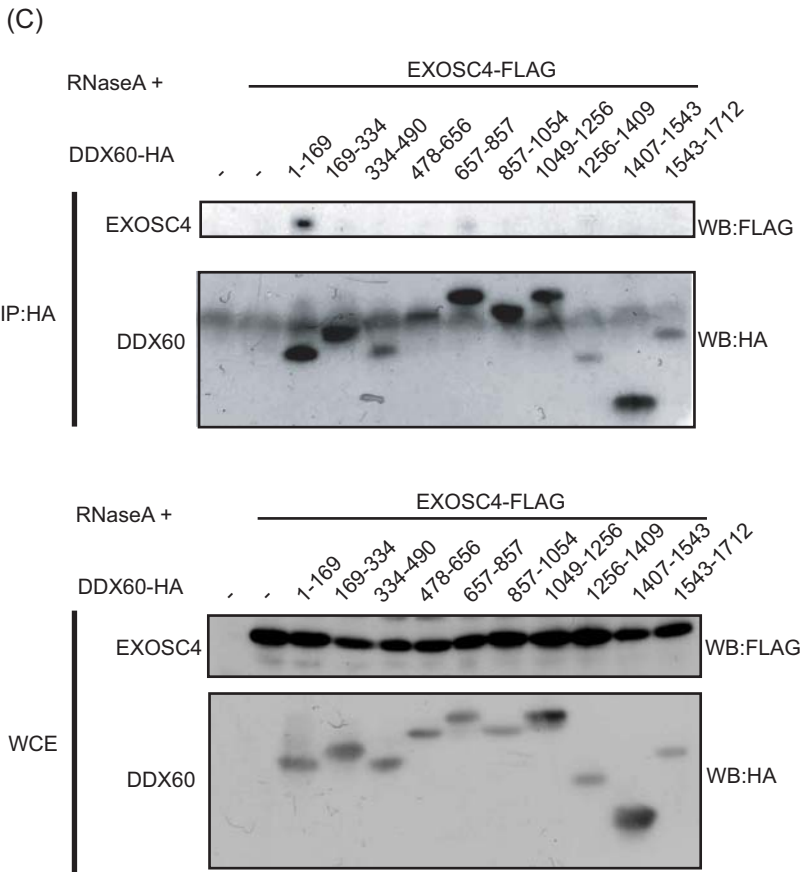
(C)
RNaseA +
EXOSC4-FLAG
DDX60-HA
1-169
169-334
334-490
478-656
657-857
857-1054
1049-1256
1256-1409
1407-1543
1543-1712
EXOSC4
WB:FLAG
IP:HA
DDX60
WB:HA
RNaseA +
EXOSC4-FLAG
DDX60-HA
EXOSC4
WB:FLAG
WCE
DDX60
WB:HA

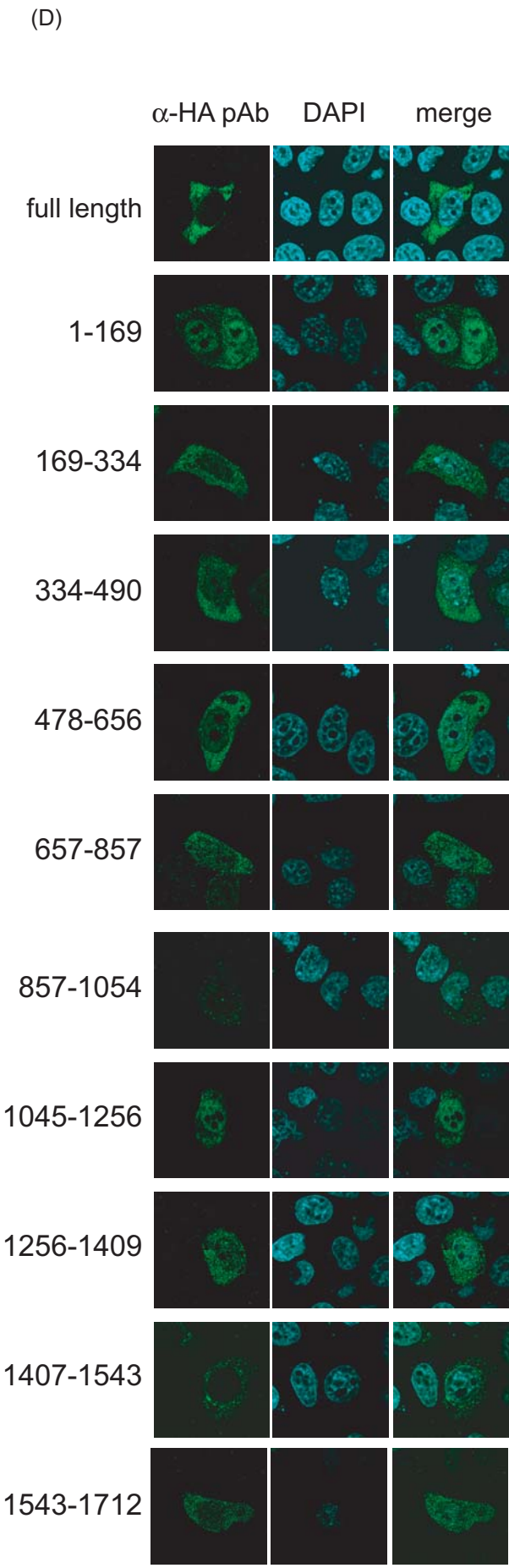
(D)
α-HA pAb
DAPI
merge
full length
1-169
169-334
334-490
478-656
657-857
857-1054
1045-1256
1256-1409
1407-1543
1543-1712

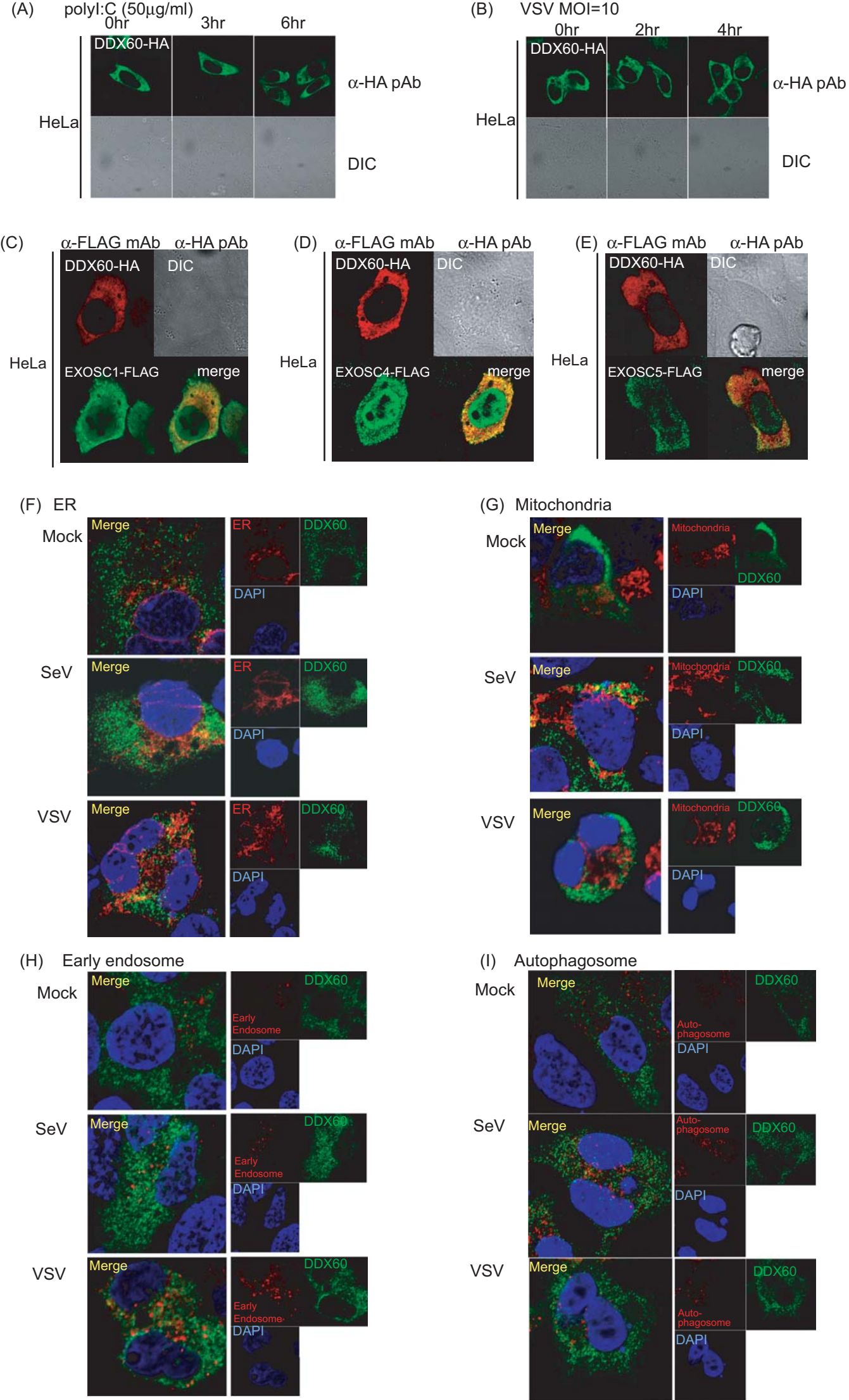
(A)
polyI:C (50μg/ml)
0hr
3hr
6hr
DDX60-HA
HeLa
α-HA pAb
DIC
(B)
VSV MOI=10
0hr
2hr
4hr
DDX60-HA
HeLa
α-HA pAb
DIC
(C)
α-FLAG mAb
α-HA pAb
DDX60-HA
DIC
HeLa
EXOSC1-FLAG
merge
(D)
α-FLAG mAb
α-HA pAb
DDX60-HA
DIC
HeLa
EXOSC4-FLAG
merge
(E)
α-FLAG mAb
α-HA pAb
DDX60-HA
DIC
HeLa
EXOSC5-FLAG
merge
(F) ER
Mock
SeV
VSV
Merge
ER
DDX60
DAPI
(G) Mitochondria
Mock
SeV
VSV
Merge
Mitochondria
DDX60
DAPI
(H) Early endosome
Mock
SeV
VSV
Merge
DDX60
Early Endosome
DAPI
(I) Autophagosome
Mock
SeV
VSV
Merge
DDX60
Auto-phagosome
DAPI

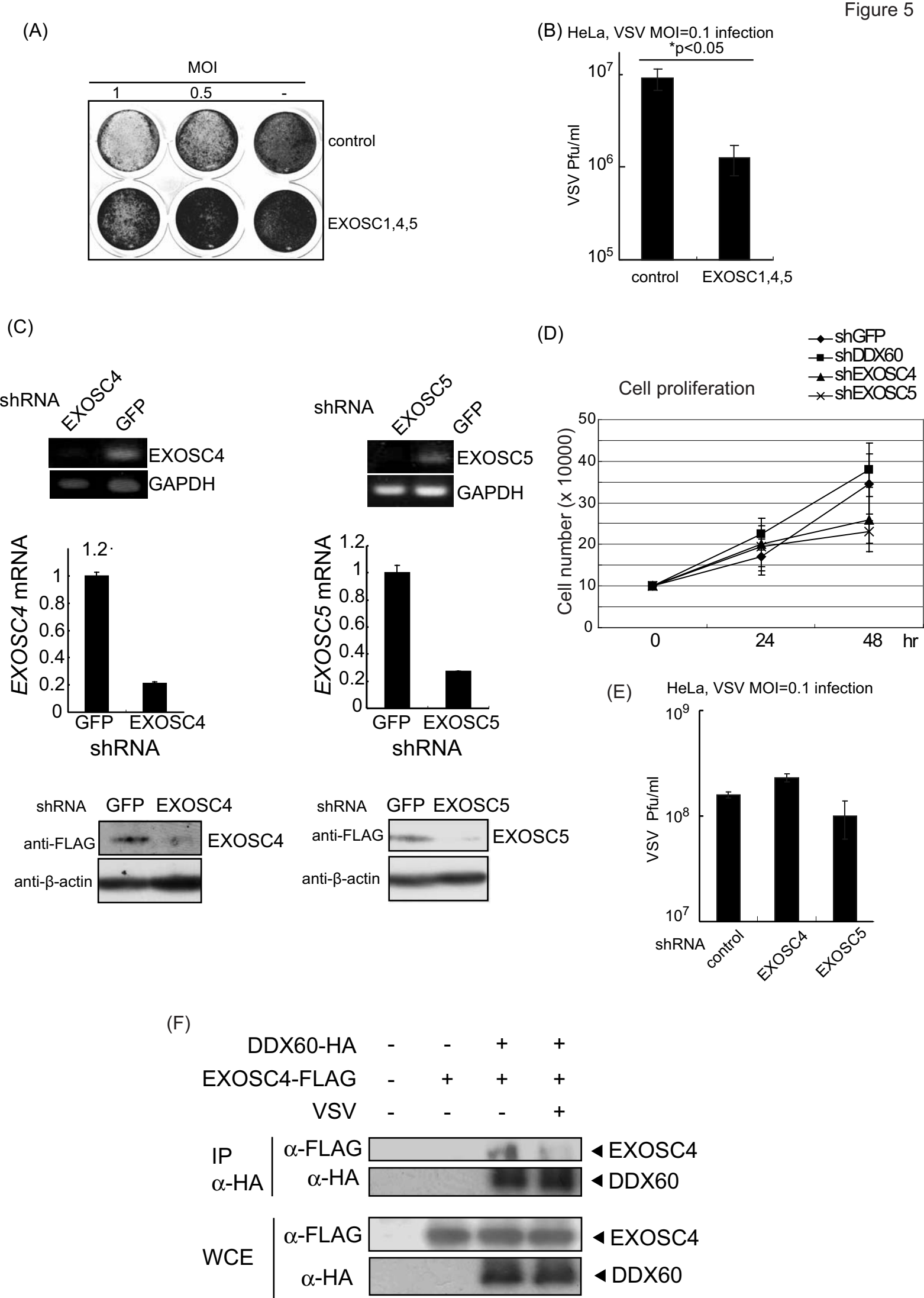
(A)
MOI
1
0.5
-
control
EXOSC1,4,5
(B) HeLa, VSV MOI=0.1 infection
*p<0.05
VSV Pfu/ml
control
EXOSC1,4,5
(C)
shRNA
EXOSC4
GFP
EXOSC4
GAPDH
EXOSC4 mRNA
shRNA
shRNA
EXOSC5
GFP
EXOSC5
GAPDH
EXOSC5 mRNA
shRNA
shRNA GFP EXOSC4
anti-FLAG
EXOSC4
anti-β-actin
shRNA GFP EXOSC5
anti-FLAG
EXOSC5
anti-β-actin
(D)
shGFP
shDDX60
shEXOSC4
shEXOSC5
Cell proliferation
Cell number (x 10000)
hr
(E)
HeLa, VSV MOI=0.1 infection
VSV Pfu/ml
shRNA
control
EXOSC4
EXOSC5
(F)
DDX60-HA
EXOSC4-FLAG
VSV
IP
α-HA
α-FLAG
α-HA
EXOSC4
DDX60
WCE
α-FLAG
α-HA
EXOSC4
DDX60

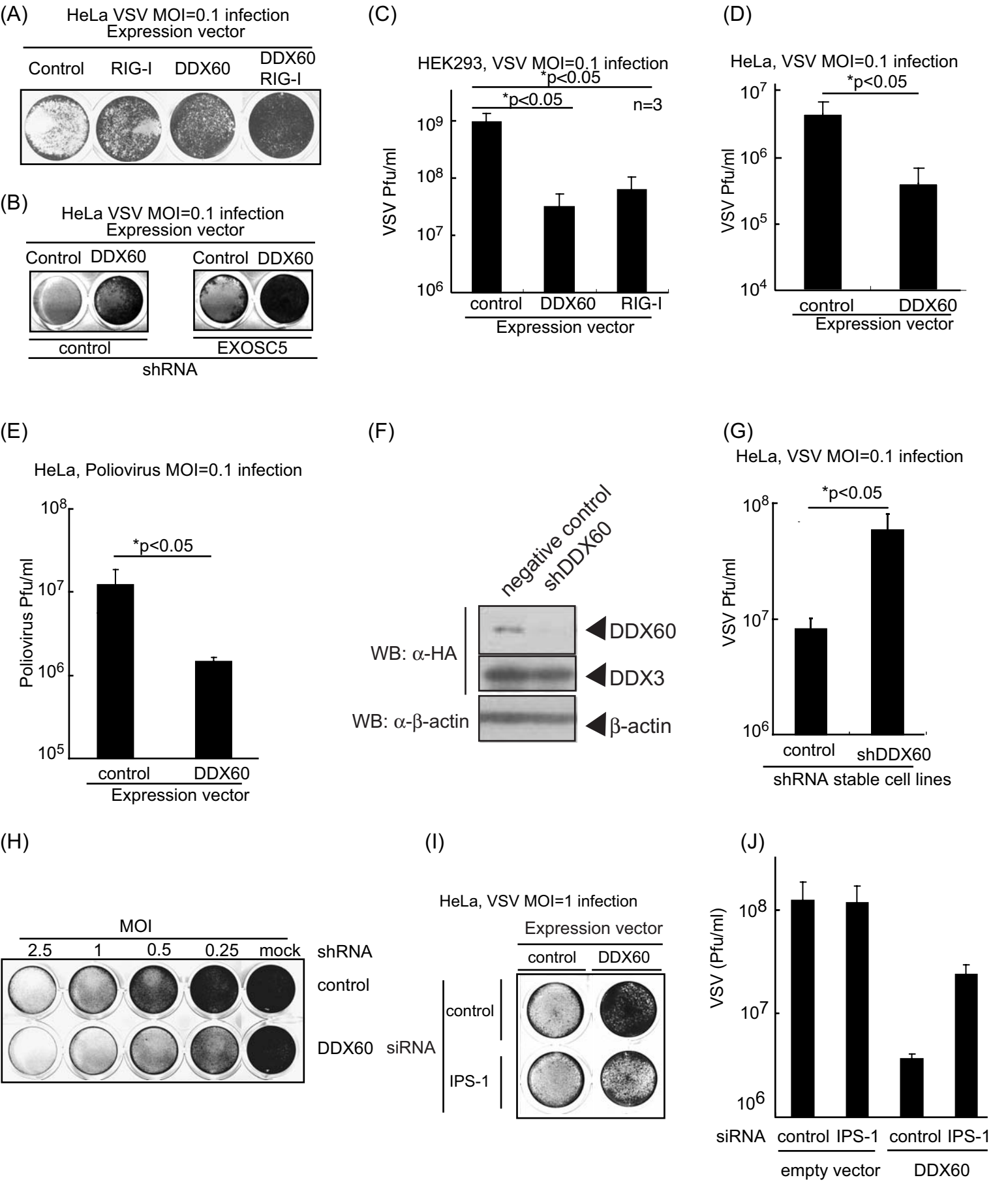
(A)
HeLa VSV MOI=0.1 infection
Expression vector
Control
RIG-I
DDX60
DDX60 RIG-I
(B)
HeLa VSV MOI=0.1 infection
Expression vector
Control DDX60
Control DDX60
control
EXOSC5
shRNA
(C)
HEK293, VSV MOI=0.1 infection
*p<0.05
*p<0.05
n=3
VSV Pfu/ml
control
DDX60
RIG-I
Expression vector
(D)
HeLa, VSV MOI=0.1 infection
*p<0.05
VSV Pfu/ml
control
DDX60
Expression vector
(E)
HeLa, Poliovirus MOI=0.1 infection
*p<0.05
Poliovirus Pfu/ml
control
DDX60
Expression vector
(F)
negative control
shDDX60
WB: α-HA
DDX60
DDX3
WB: α-β-actin
β-actin
(G)
HeLa, VSV MOI=0.1 infection
*p<0.05
VSV Pfu/ml
control
shDDX60
shRNA stable cell lines
(H)
MOI
2.5
1
0.5
0.25
mock
shRNA
control
DDX60
siRNA
(I)
HeLa, VSV MOI=1 infection
Expression vector
control
DDX60
control
IPS-1
(J)
VSV (Pfu/ml)
siRNA
control
IPS-1
control
IPS-1
empty vector
DDX60

Figure 7

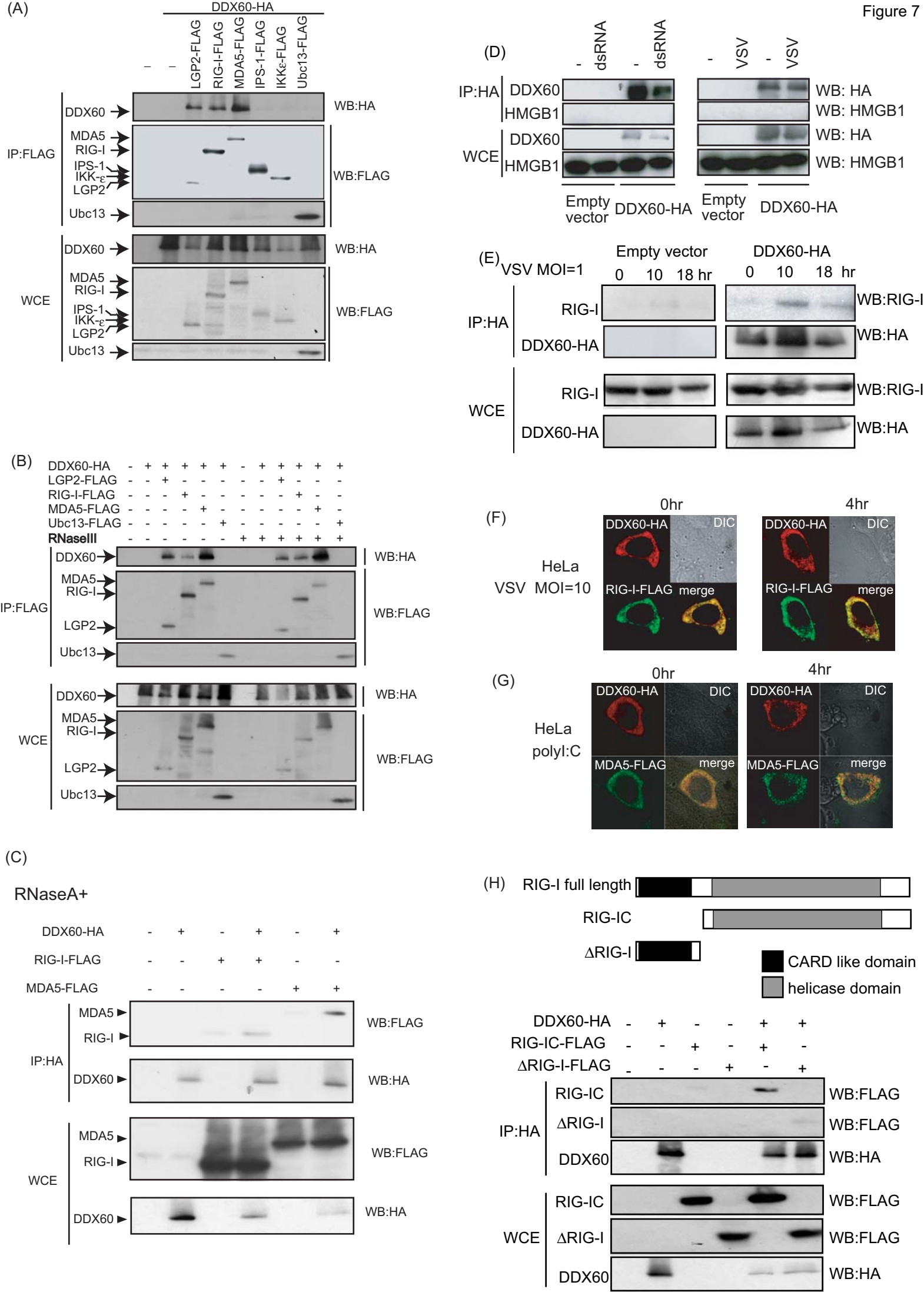
(A)
DDX60-HA
LGP2-FLAG
RIG-I-FLAG
MDA5-FLAG
IPS-1-FLAG
IKKε-FLAG
Ubc13-FLAG
IP:FLAG
DDX60
MDA5
RIG-I
IPS-1
IKK-ε
LGP2
Ubc13
WB:HA
WB:FLAG
WCE
(B)
DDX60-HA
LGP2-FLAG
RIG-I-FLAG
MDA5-FLAG
Ubc13-FLAG
RNaseIII
(C)
RNaseA+
(D)
dsRNA
VSV
IP:HA
WCE
DDX60
HMGB1
WB: HA
WB: HMGB1
Empty vector
DDX60-HA
(E)
VSV MOI=1
0 10 18 hr
RIG-I
WB:RIG-I
WB:HA
(F)
HeLa
VSV MOI=10
0hr
4hr
DIC
merge
(G)
HeLa
polyI:C
MDA5-FLAG
(H)
RIG-I full length
RIG-IC
ΔRIG-I
CARD like domain
helicase domain
RIG-IC-FLAG
ΔRIG-I-FLAG

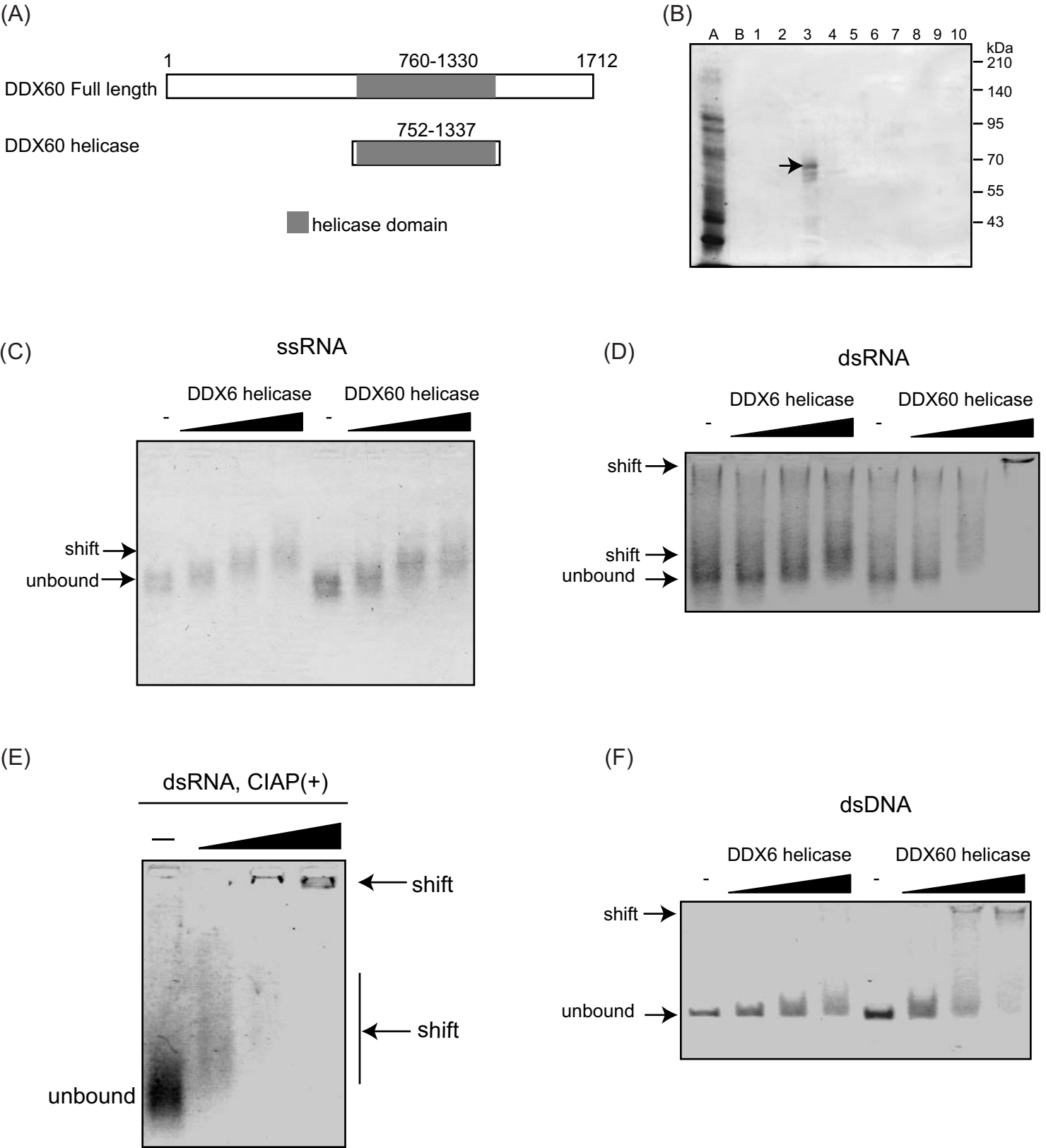
(A)
1
760-1330
1712
DDX60 Full length
752-1337
DDX60 helicase
helicase domain
(B)
A B 1 2 3 4 5 6 7 8 9 10
kDa
210
140
95
70
55
43
(C)
ssRNA
DDX6 helicase
DDX60 helicase
shift
unbound
(D)
dsRNA
DDX6 helicase
DDX60 helicase
shift
shift
unbound
(E)
dsRNA, CIAP(+)
shift
shift
unbound
(F)
dsDNA
DDX6 helicase
DDX60 helicase
shift
unbound

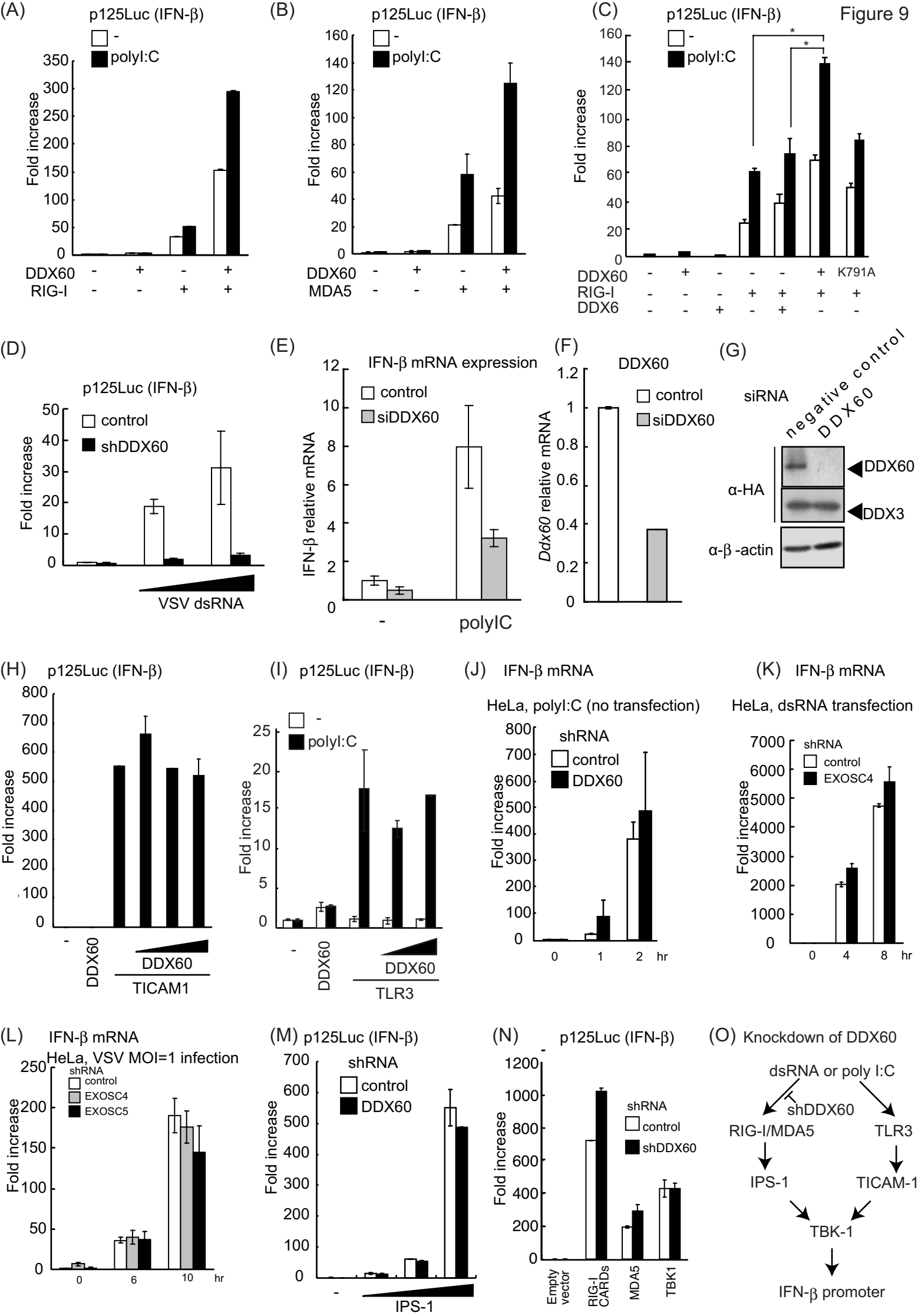
(A)
p125Luc (IFN-β)
-
polyI:C
Fold increase
DDX60
RIG-I
(B)
p125Luc (IFN-β)
-
polyI:C
Fold increase
DDX60
MDA5
(C)
p125Luc (IFN-β)
-
polyI:C
Fold increase
DDX60
RIG-I
DDX6
K791A
(D)
p125Luc (IFN-β)
control
shDDX60
Fold increase
VSV dsRNA
(E)
IFN-β mRNA expression
control
siDDX60
IFN-β relative mRNA
-
polyIC
(F)
DDX60
control
siDDX60
Ddx60 relative mRNA
(G)
siRNA
negative control
DDX60
DDX60
DDX3
α-HA
α-β -actin
(H)
p125Luc (IFN-β)
Fold increase
DDX60
TICAM1
(I)
p125Luc (IFN-β)
-
polyI:C
Fold increase
DDX60
TLR3
(J)
IFN-β mRNA
HeLa, polyI:C (no transfection)
shRNA
control
DDX60
Fold increase
hr
(K)
IFN-β mRNA
HeLa, dsRNA transfection
shRNA
control
EXOSC4
Fold increase
hr
(L)
IFN-β mRNA
HeLa, VSV MOI=1 infection
shRNA
control
EXOSC4
EXOSC5
Fold increase
hr
(M)
p125Luc (IFN-β)
shRNA
control
DDX60
Fold increase
IPS-1
(N)
p125Luc (IFN-β)
shRNA
control
shDDX60
Fold increase
Empty vector
RIG-I CARDs
MDA5
TBK1
(O)
Knockdown of DDX60
dsRNA or poly I:C
shDDX60
RIG-I/MDA5
TLR3
IPS-1
TICAM-1
TBK-1
IFN-β promoter

Figure 10

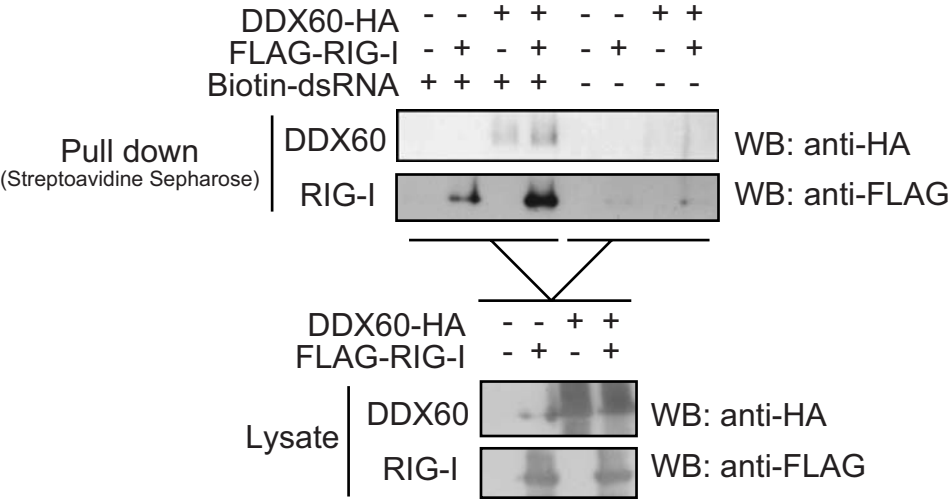
DDX60-HA - - + + - - + +
FLAG-RIG-I - + - + - + - +
Biotin-dsRNA + + + + - - - -
Pull down
(Streptoavidine Sepharose)
DDX60
RIG-I
WB: anti-HA
WB: anti-FLAG
DDX60-HA - - + +
FLAG-RIG-I - + - +
Lysate
DDX60
RIG-I
WB: anti-HA
WB: anti-FLAG

Figure 11

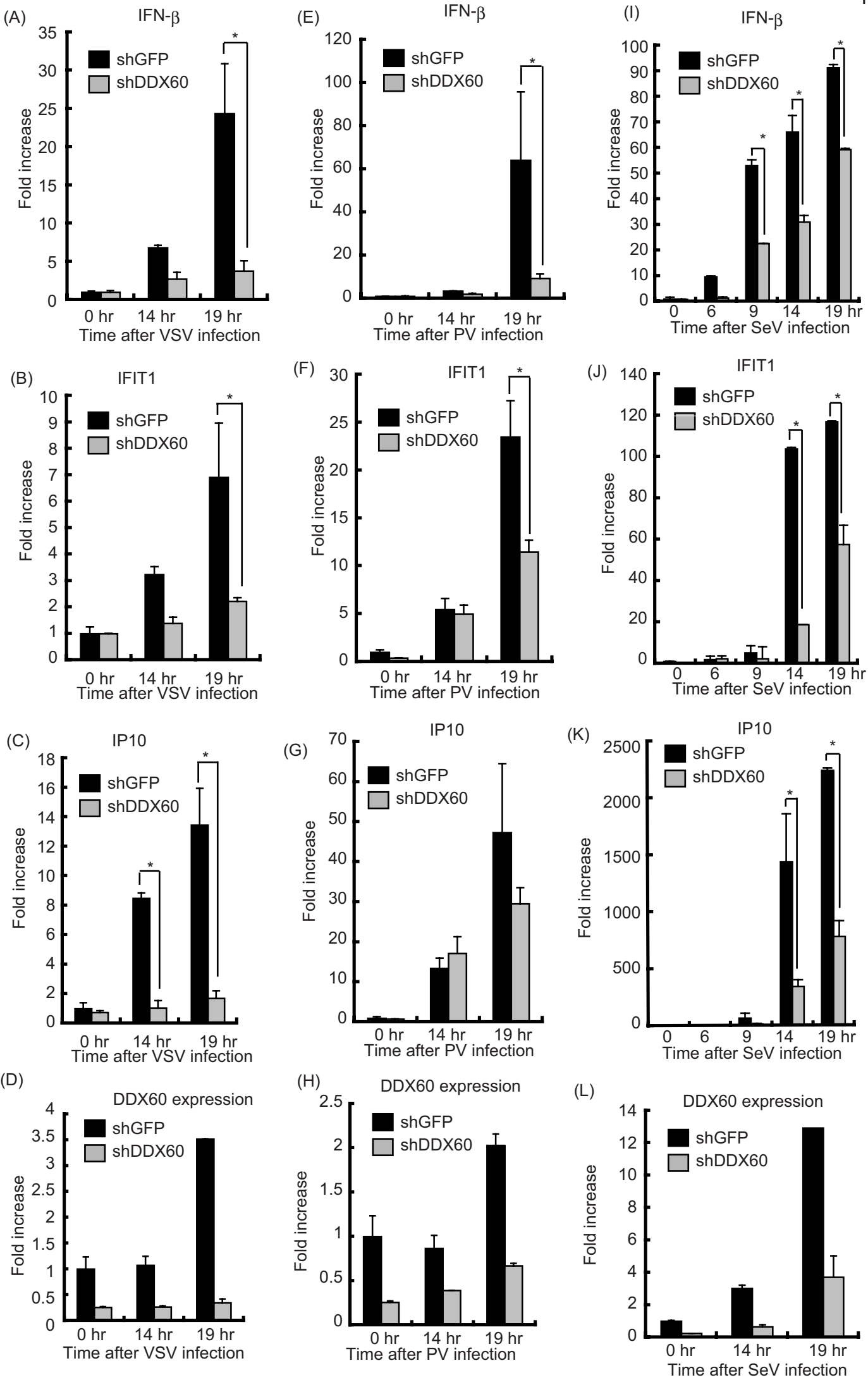
(A)
IFN-β
shGFP
shDDX60
Fold increase
0 hr
14 hr
19 hr
Time after VSV infection
(E)
IFN-β
shGFP
shDDX60
Fold increase
0 hr
14 hr
19 hr
Time after PV infection
(I)
IFN-β
shGFP
shDDX60
Fold increase
0
6
9
14
19 hr
Time after SeV infection
(B)
IFIT1
shGFP
shDDX60
Fold increase
0 hr
14 hr
19 hr
Time after VSV infection
(F)
IFIT1
shGFP
shDDX60
Fold increase
0 hr
14 hr
19 hr
Time after PV infection
(J)
IFIT1
shGFP
shDDX60
Fold increase
0
6
9
14
19 hr
Time after SeV infection
(C)
IP10
shGFP
shDDX60
Fold increase
0 hr
14 hr
19 hr
Time after VSV infection
(G)
IP10
shGFP
shDDX60
Fold increase
0 hr
14 hr
19 hr
Time after PV infection
(K)
IP10
shGFP
shDDX60
Fold increase
0
6
9
14
19 hr
Time after SeV infection
(D)
DDX60 expression
shGFP
shDDX60
Fold increase
0 hr
14 hr
19 hr
Time after VSV infection
(H)
DDX60 expression
shGFP
shDDX60
Fold increase
0 hr
14 hr
19 hr
Time after PV infection
(L)
DDX60 expression
shGFP
shDDX60
Fold increase
0 hr
14 hr
19 hr
Time after SeV infection

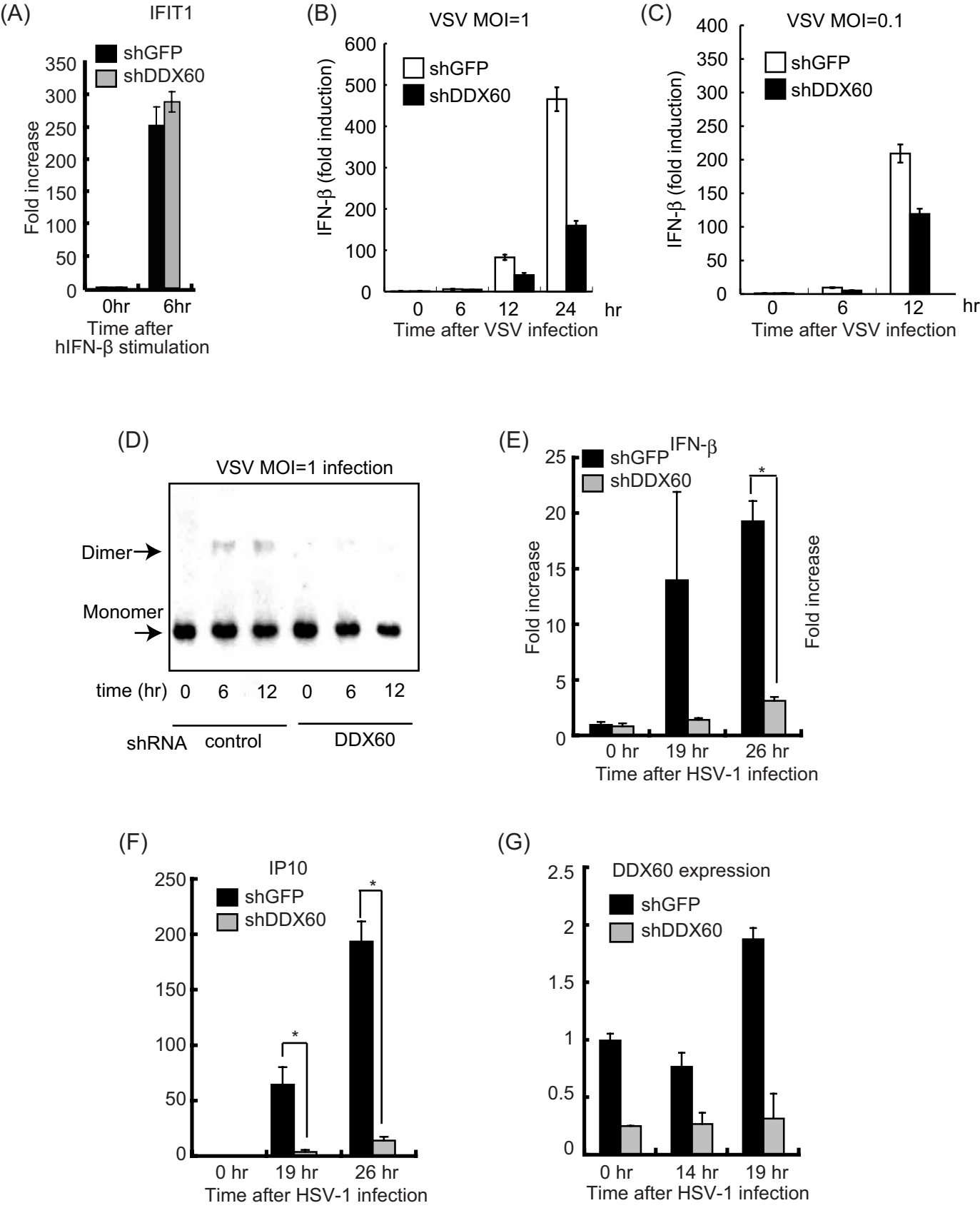
(A)
IFIT1
shGFP
shDDX60
Fold increase
0hr
6hr
Time after
hIFN-β stimulation
(B)
VSV MOI=1
shGFP
shDDX60
IFN-β (fold induction)
Time after VSV infection
hr
(C)
VSV MOI=0.1
shGFP
shDDX60
IFN-β (fold induction)
Time after VSV infection
hr
(D)
VSV MOI=1 infection
Dimer
Monomer
time (hr) 0 6 12 0 6 12
shRNA control DDX60
(E)
IFN-β
shGFP
shDDX60
Fold increase
Fold increase
0 hr 19 hr 26 hr
Time after HSV-1 infection
(F)
IP10
shGFP
shDDX60
0 hr 19 hr 26 hr
Time after HSV-1 infection
(G)
DDX60 expression
shGFP
shDDX60
0 hr 14 hr 19 hr
Time after HSV-1 infection